

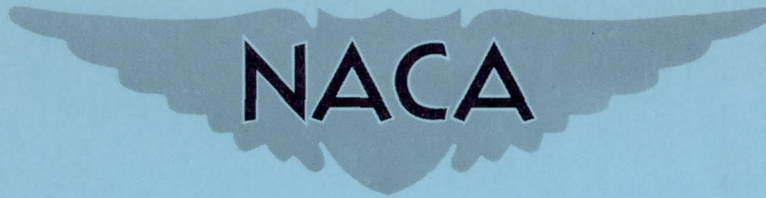
**CONFIDENTIAL**

Copy 309

**SECURITY INFORMATION**

RM A52F13

NACA RM A52F13



# RESEARCH MEMORANDUM

CONTROL EFFECTIVENESS AND HINGE-MOMENT CHARACTERISTICS AT  
LOW-SPEED OF LARGE-CHORD, HORN-BALANCED, FLAP-TYPE  
CONTROLS ON A TRIANGULAR WING OF ASPECT RATIO 2

THIS DOCUMENT ON LOAN FROM THE FILES OF By Jules B. Dods, Jr.

NATIONAL ADVISORY COMMITTEE FOR AERONAUTICS  
LANGLEY AERONAUTICAL LABORATORY  
LANGLEY FIELD, HAMPTON, VIRGINIA  
Ames Aeronautical Laboratory  
Moffett Field, Calif.

CLASSIFICATION CHANGED TO UNCLASSIFIED

RETURN TO THE OFFICE OF \_\_\_\_\_

AUTHORITY J.W. CROWLEY DATE: 10-12-54

REMARKS FOR PUBLICATION SHOULD BE ADDRESSED  
AS FOLLOWS:

CHANGE NO. 2746

WHL

NATIONAL ADVISORY COMMITTEE FOR AERONAUTICS  
1512 H STREET, N. W.  
WASHINGTON 25, D. C.

CLASSIFIED DOCUMENT

This material contains information affecting the National Defense of the United States within the meaning of the espionage laws, Title 18, U.S.C., Secs. 793 and 794, the transmission or revelation of which in any manner to an unauthorized person is prohibited by law.

## NATIONAL ADVISORY COMMITTEE FOR AERONAUTICS

WASHINGTON

August 18, 1952

**CONFIDENTIAL**

**CONFIDENTIAL**  
**SECURITY INFORMATION**

NATIONAL ADVISORY COMMITTEE FOR AERONAUTICS

RESEARCH MEMORANDUM

CONTROL EFFECTIVENESS AND HINGE-MOMENT CHARACTERISTICS AT

LOW SPEED OF LARGE-CHORD, HORN-BALANCED, FLAP-TYPE

CONTROLS ON A TRIANGULAR WING OF ASPECT RATIO 2

By Jules B. Dods, Jr.

## SUMMARY

Large-chord flap-type controls with swept-back hinge lines and with various sizes and shapes of horn balances were investigated on a triangular wing of aspect ratio 2. The effects of changes in the following were examined: shielding of the horn balance, percentage of horn balance, trailing-edge thickness, flap nose seal, contour of the horn balance, and Reynolds number. One of the controls which had a nearly optimum balance at low speed was compared with several other types of controls on triangular wings and with an all-movable triangular-wing control for two hinge-line positions.

The results of the investigation indicated that a large-chord control surface with a swept-back hinge line could be satisfactorily balanced aerodynamically at low speeds by means of a horn balance. It was also found that the rate of change of hinge-moment coefficient with elevator deflection varied by a smaller amount than the rate of change of hinge-moment coefficient with angle of attack with changes in the amount of horn balance, the degree of horn shielding, and the trailing-edge thickness of the control.

## INTRODUCTION

The development of aircraft capable of high-speed flight has introduced new problems of stability and control. One such problem consists of providing controls on plan forms suitable for flight at transonic and supersonic speeds which have adequate effectiveness and which have reasonably small control forces. The problem of reducing control forces has become so severe that designers have had to resort

**CONFIDENTIAL**  
**SECURITY INFORMATION**

to the use of irreversible power boost systems. Despite the use of such power boost systems it appears desirable to develop control surfaces with aerodynamic balances to reduce hinge moments for the following reasons: (1) to provide some measure of emergency control by the use of manual override systems in the event of the failure of the power boost system; (2) to permit the reduction of booster power requirements, and thus booster size and weight; and (3) to reduce torsional deformation of control surfaces.

The present tests are part of a general investigation being conducted by the NACA of various types of balanced and unbalanced controls particularly applicable to triangular plan forms (references 1 through 14). The primary purpose of the present investigation was to determine experimentally the low-speed effectiveness and particularly the hinge-moment parameters of a control on a triangular wing<sup>1</sup> which had various horn balances and which had the hinge line swept back 40°. The control was designed with a large ratio of the area behind the hinge line to the total wing area so that the lift effectiveness would approach that of an all-movable surface. Thus, it is not to be inferred that smaller controls could not be similarly balanced. The model had various horn balances which varied both in plan form and in contour. Results are presented for the flap nose sealed and unsealed, for thickened trailing edges of the flap, and for several values of the Reynolds number. A secondary purpose of the investigation was to compare the results obtained for one of the controls which was deemed to have good balancing characteristics at low speeds with the characteristics of a wing having plain flaps (references 1 and 2), a wing having a half-delta tip control (reference 4), and an all-movable surface (reference 3).<sup>2</sup>

The scope of the present investigation was limited to Mach numbers up to 0.29 for these preliminary tests. The tests were conducted in one of the Ames 7- by 10-foot wind tunnels.

#### NOTATION

$C_D$  drag coefficient  $\left( \frac{D}{qS} \right)$

---

<sup>1</sup>Although the term "wing" is used throughout the report for generality, it is probable that these wing-flap combinations would be more applicable as a horizontal or a vertical tail.

<sup>2</sup>The pitching-moment coefficients of reference 3 were used to compute the hinge-moment coefficients of the all-movable surface.

---

- $C_h$  hinge-moment coefficient  $\left(\frac{H}{2M_A q}\right)$   
(For the all-movable surface  $S\bar{c}$  replaces  $2M_A$ .)
- $C_L$  lift coefficient  $\left(\frac{L}{qS}\right)$
- $C_m$  pitching-moment coefficient  $\left(\frac{M_1}{qS\bar{c}}\right)$
- $K_h$  hinge-moment factor (used for comparison of widely different types of controls)  $\left(\frac{H}{qS\bar{c}}\right)$
- $a$  speed of sound, feet per second
- $b$  twice span of the semispan model, measured perpendicular to the plane of symmetry, feet
- $c$  chord of the model measured parallel to the plane of symmetry, feet
- $\bar{c}$  mean aerodynamic chord  $\left(\frac{\int_0^{b/2} c^2 dy}{\int_0^{b/2} c dy}\right)$ , feet
- $D$  drag, pounds
- $H$  hinge moment, foot-pounds
- $\frac{h}{t}$  ratio of the thickness of the flap measured at the trailing edge to the thickness of the airfoil measured at the 67-percent-chord station
- $L$  lift, pounds
- $M$  Mach number  $\left(\frac{V}{a}\right)$
- $M_1$  pitching moment about one-quarter  $\bar{c}$ , foot-pounds
- $M_A$  moment about the hinge line of the flap area behind the hinge line, feet cubed
- $q$  free-stream dynamic pressure, pounds per square foot

- R Reynolds number  $\left(\frac{\rho V \bar{c}}{\mu}\right)$
- S semispan-model area, square feet
- V velocity of free stream, feet per second
- y lateral distance normal to the plane of symmetry, feet
- $\alpha$  corrected angle of attack, degrees
- $\Delta$  increment due to the tunnel walls
- $\delta$  flap deflection measured in a plane normal to the flap hinge line, degrees (except as noted)
- $\mu$  absolute viscosity, slugs per foot-second
- $\rho$  density of air, slugs per cubic foot

## Subscripts

- w wing or airfoil
- f flap

## Parameters

$$C_{h\alpha} = \left(\frac{\partial C_h}{\partial \alpha}\right)_{\delta=0}, \text{ per degree (measured through } \alpha = 0)$$

$$C_{h\delta} = \left(\frac{\partial C_h}{\partial \delta}\right)_{\alpha=0}, \text{ per degree (measured through } \delta = 0)$$

$$C_{L\alpha} = \left(\frac{\partial C_L}{\partial \alpha}\right)_{\delta=0}, \text{ per degree (measured through } \alpha = 0)$$

$$C_{L\delta} = \left(\frac{\partial C_L}{\partial \delta}\right)_{\alpha=0}, \text{ per degree (measured through } \delta = 0)$$

$$K_{h\alpha} = \left( \frac{\partial K_h}{\partial \alpha} \right)_{\delta=0}, \text{ per degree (measured through } \alpha = 0)$$

$$K_{h\delta} = \left( \frac{\partial K_h}{\partial \delta} \right)_{\alpha=0}, \text{ per degree (measured through } \delta = 0)$$

The subscripts outside the parentheses represent the factor held constant for the measurement of the parameters.

### MODEL AND APPARATUS

The wing tested was a triangular, semispan, reflection-plane model of aspect ratio 2 having the leading edge swept back  $63.43^\circ$  and having a modified NACA 0005 section (table I) parallel to the free stream. The modification consisted of replacing the normal profile with straight lines back of the 67-percent-chord station. The geometry of the model is shown in figure 1, and photographs of the model are given in figure 2. The hinge line intersected the root chord at the 50-percent-chord point and was swept back  $40^\circ$ , forming a flap which had an area behind the hinge line which was 56.93 percent of the total wing area. The portion of the flap ahead of the hinge line and the fixed portion (apex) of the wing were constructed so as to permit the variation of the sizes and shapes of the horn balances. The percentage of horn balance is defined as the ratio of the control area ahead of the hinge line to the control area behind the hinge line multiplied by 100. These balances in conjunction with the invariant flap area behind the hinge line formed controls A, B, C, D, and E as shown in figure 1. The horn balances on controls A and B were relieved in order to eliminate the interference that would otherwise occur between the fixed portion of the model and the horn balance as the controls were deflected. The normal configuration of the controls was with the flap nose unsealed, the normal-airfoil-contour horn balance, and with normal airfoil trailing-edge thickness,  $h/t = 0$ .

Control A had two additional values of trailing-edge thickness,  $h/t = 0.5$  and  $h/t = 1.0$ . (One trailing-edge thickness was equal to one-half the normal airfoil thickness at the 67-percent-chord station, and the other trailing-edge thickness was equal to the airfoil thickness at that station.) These variations in the trailing-edge thickness of the flap were formed by straight-sided wedges which extended from the 67-percent-chord station to the trailing edge.

Control C had both a sealed and an unsealed flap nose, and had both a normal-airfoil-contour horn balance and a thin contour horn balance.

The details of the flap nose seal are shown in section A-A, figure 1. The thin horn contour was formed by ellipses. The minor axes equaled the thickness of the wing at a reference line which was perpendicular to the hinge line and which was 24.69 inches from the plane of symmetry measured along the hinge line. The lengths of the semimajor axes were measured between the reference line and the inner end of the horn of control C along radial lines from the wing tip. A free fairing across these ellipses perpendicular to the hinge line was used to join the normal airfoil contour at the hinge line. The thin contour control C can be seen in figures 2(a) to 2(d).

The control hinge moments were measured by means of a resistance-type electric strain gage.

#### CORRECTIONS TO DATA

The data have been corrected for the effects of tunnel-wall interference by the method of reference 15. The corrections added to the data were as follows:

$$\Delta\alpha = 0.856 C_{L_{w+f}} + 0.1834 C_{L_w}$$

$$(\Delta C_m)_{w+f} = 0.00753 C_{L_{w+f}}$$

$$\Delta C_D = 0.0169 C_{L_{w+f}}^2$$

$$\Delta C_h = 0.0092 C_{L_{w+f}}$$

The lift coefficient was corrected by multiplying the uncorrected value by 0.992.

#### RESULTS AND DISCUSSION

##### Presentation of Results

The variations of the lift and hinge-moment coefficients with angle of attack and with flap deflection are presented in figures 3 through 11 for controls A, B, C, D, and E at a Mach number of 0.18 and a Reynolds number of 5,000,000. Data are shown for various conditions of the flap nose gap, horn-balance contour, and trailing-edge thickness. The pitching-moment and drag coefficients are also presented for control A ( $h/t = 0$ ); (figs. 3(d), 3(e), and 3(f)). The changes in the hinge-moment

parameters for all the controls (A through E) are summarized in figure 12. The effect of changes in the Reynolds number is given in figure 13 for control A ( $h/t = 0$ ). Summary lift and hinge-moment data for all controls tested are given for zero flap deflection in figures 14(a) and 14(b). A list of the lift and hinge-moment parameters for the various controls tested is also given in table II. A comparison is made in figures 15(a) and 15(b) of the lift and hinge-moment parameters of control A ( $h/t = 0$ ) with those of unbalanced controls (references 1 and 2), a balanced control (reference 4), and an all-movable surface (reference 3).

### Discussion of Experimental Results

The following discussion is concerned primarily with the hinge-moment parameters because, as shown in figures 3(a) to 11(a) and in table II, the effects of the various modifications on the lift parameters were practically negligible. The slope parameters measured with respect to  $\delta$  given in table II are for  $\delta$  measured normal to the hinge line. The stalling characteristics varied slightly as can be seen from the summary in figure 14(a). The horn-balanced controls with the horn-gap direction parallel to the free stream will be referred to as the unshielded horn controls, and the horn-balanced controls with the horn-gap direction perpendicular to the hinge line will be referred to as the shielded horn controls.

Effect of percent of horn balance.- The effect of changes in the percentage of horn balancing of the control upon the hinge-moment parameters is shown in figure 12. As would be expected, relatively small increases in the amount of horn balance produce sizable reductions in both of the hinge-moment parameters,  $C_{h\alpha}$  and  $C_{h\delta}$ . The increment of  $C_{h\delta}$  obtained by increasing the horn balance over the range of percentage balances tested was about the same for either the unshielded or the shielded horn balances; however, the incremental effect on  $C_{h\alpha}$  was about twice as great for the unshielded balance as for the shielded balance. It should be noted that the differential increments of  $C_{h\alpha}$  and  $C_{h\delta}$  obtained for a given change in the percentage horn balance of the unshielded horn could be of use to the designer in altering the ratio  $C_{h\alpha}/C_{h\delta}$ .

Effect of shielding the horn balance.- The effect of shielding the horn balance upon the hinge-moment parameter is also shown in figure 12. The effect of shielding the horn at a constant value of the percentage balance was to increase the numerical value of  $C_{h\alpha}$ . The amount of

increase was a function of the percentage balance; the incremental increase in  $C_{h\alpha}$  was about two and one-half times as great at 22.72-percent balance as it was at 16.98-percent balance. The effect of shielding the horn upon  $C_{h\delta}$  was not measurable for 16.98-percent balance, but a small increase in  $C_{h\delta}$  was evident at 22.72-percent balance. These results indicate that  $C_{h\alpha}$  and  $C_{h\delta}$  may be differentially controlled by changing the amount of horn shielding, at least within the limits of the present investigation.

Effect of horn-balance contour.- The effect of changing the shape of the horn balance from the normal airfoil contour to a thin contour (see model description) was found to be moderately small for the shielded horn balance. As shown in figure 12, the absolute value of  $C_{h\alpha}$  was only increased from -0.0018 to -0.0019 while  $C_{h\delta}$  was increased from -0.0030 to -0.0036. Thus, it is seen that changes in the horn-balance contour also provide a method for differentially changing the hinge-moment parameters. It is interesting to note that thinning the horn-balance contour was the only variable investigated which produced a larger change in  $C_{h\delta}$  than in  $C_{h\alpha}$ .

Effect of trailing-edge thickness.- The effect of changes in the trailing-edge thickness, ( $h/t$ ), is given in figure 12. The trailing-edge thickness was varied only for one value of the percentage horn balance and only for the unshielded horn balance. A change in the trailing-edge thickness from  $h/t = 0$  to  $h/t = 0.5$  increased the numerical value of  $C_{h\alpha}$  about three times as much as  $C_{h\delta}$  was increased. A further change in the trailing-edge thickness from  $h/t = 0.5$  to 1.0 resulted in approximately equal changes in  $C_{h\alpha}$  and  $C_{h\delta}$ .

Effect of flap-nose seal.- The effect of sealing the flap nose as shown in figure 12 was found only for the shielded horn balance. The effect of sealing the flap nose was negligible on  $C_{h\alpha}$  and reduced  $C_{h\delta}$  by only a small amount.

Effect of Reynolds number.- The effects upon the lift and the hinge-moment coefficients of increasing the Reynolds number from 3,000,000 to 8,000,000, for Mach numbers of 0.10 and 0.29, respectively, are shown in figure 13 for several deflections of control A ( $h/t = 0$ ). The effects of changes in the Reynolds number in the range tested were negligible.

Comparison of Control A ( $h/t = 0$ ) With Unbalanced,  
Balanced, and All-Movable Controls

A comparison of the aerodynamic characteristics of control A ( $h/t = 0$ ) with those of the unbalanced controls of references 1 and 2,

the balanced control of reference 4, and the all-movable surface of reference 3 is presented in figure 15. The lift-effectiveness parameters are presented in figure 15(a), and the hinge-moment parameters are given in figure 15(b). Two positions of the hinge line are considered for the all-movable surface: one at 45-percent  $\bar{c}$  which would provide approximately minimum hinge-moment coefficients at transonic speeds, and another at 51-percent  $\bar{c}$  which would provide minimum hinge-moment coefficients at supersonic speeds.

The conventional hinge-moment parameters  $C_{h\alpha}$  and  $C_{h\delta}$  in figure 15(b) do not provide a ready comparison of the controls from a hinge-moment standpoint, however, since the hinge-moment coefficients for each control are a function of the size of the control as well as the hinge moment. Because of the large differences in the size of the controls being compared for the given wing plan form, a better comparison of the hinge moment per unit deflection would be obtained utilizing a parameter that involved the wing geometry (as is the case for the lift-effectiveness parameters  $C_{L\alpha}$  and  $C_{L\delta}$ ) rather than the control geometry. Hence, the parameters  $K_{h\alpha}$  and  $K_{h\delta}$  are introduced in order to provide a direct comparison of the hinge moments per unit deflection for these controls on a wing of a given size at a given dynamic pressure. For  $K_{h\alpha}$  and  $K_{h\delta}$ , the value of the cubic-foot factor used to reduce the hinge moments to nondimensional form was arbitrarily chosen as  $S\bar{c}$ . The values of  $K_{h\alpha}$  and  $K_{h\delta}$  for the various controls are also presented in figure 15(b). These data indicate that the variations of hinge moment per unit angular change with Mach number for the all-movable controls are considerably greater than that for the plain flap controls of references 1 and 2 and for the half-delta tip control of reference 4. The all-movable surface may, of course, be completely balanced at any one value of the Mach number by simply locating the hinge line at the center of pressure for that Mach number. The large increment in hinge moment between subsonic and supersonic Mach numbers, however, would not be greatly affected by changes in the hinge-line position. Although data for control A ( $h/t = 0$ ) are not available throughout the Mach number range, the low-speed data indicate that, at least for one value of the Mach number, the hinge-moment characteristics of this control compare favorably with those of the other controls shown.

#### CONCLUSIONS

The results of an experimental wind-tunnel investigation at low speed to determine the lift effectiveness and the hinge-moment parameters of several large-chord horn-balanced controls on a triangular wing indicate the following:

1. The hinge-moment parameters  $C_{h\alpha}$  and  $C_{h\delta}$  may be controlled differentially by changing the amount of horn balance for the unshielded horn control and by changing the degree of horn shielding.
2. The effect of changing the horn-balance contour of the shielded horn control from the normal airfoil contour to a thinner elliptical contour was moderately small.
3. Increasing the trailing-edge thickness of the unshielded horn control from  $h/t = 0$  to  $h/t = 0.5$  changed  $C_{h\alpha}$  about three times as much as it changed  $C_{h\delta}$ . Further increases in trailing-edge thickness to  $h/t = 1.0$  resulted in approximately equal changes in the hinge-moment parameters.
4. Sealing the flap-nose gap of the shielded horn control resulted in a negligible change in  $C_{h\alpha}$  and reduced  $C_{h\delta}$  by only a small amount.
5. The effects upon the lift and hinge-moment coefficients of increasing the Reynolds number from 3,000,000 to 8,000,000 were negligible.

In addition, a comparison with data for other types of controls indicates that the large-chord flap-type control with a swept-back hinge line and a horn balance can be adequately balanced at low speeds.

Ames Aeronautical Laboratory  
National Advisory Committee for Aeronautics  
Moffett Field, Calif.

#### REFERENCES

1. Stephenson, Jack D., and Amuedo, Arthur R.: Tests of a Triangular Wing of Aspect Ratio 2 in the Ames 12-Foot Pressure Wind Tunnel. II - The Effectiveness and Hinge Moments of a Constant-Chord Plain Flap. NACA RM A8E03, 1948.
2. Mitcham, Grady L., Stevens, Joseph E., and Norris, Harry P.: Aerodynamic Characteristics and Flying Qualities of a Tailless Triangular-Wing Airplane Configuration as Obtained From Flights of Rocket-Propelled Models at Transonic and Low Supersonic Speeds. NACA RM L9L07, 1950.

3. Smith, Donald W., and Heitmeyer, John C.: Lift, Drag, and Pitching Moment of Low-Aspect-Ratio Wings at Subsonic and Supersonic Speeds - Plane Triangular Wing of Aspect Ratio 2 With NACA 0005-63 Section. NACA RM A50K21, 1951.
4. Martz, C. William, and Church, James D.: Flight Investigation at Subsonic, Transonic, and Supersonic Velocities of the Hinge-Moment Characteristics, Lateral-Control Effectiveness, and Wing Damping in Roll of a 60° Swept-Back Delta Wing With Half-Delta Tip Ailerons. NACA RM L51G18, 1951.
5. Bates, William R.: Low-Speed Static Longitudinal Stability Characteristics of a Canard Model Having a 60° Triangular Wing and Horizontal Tail. NACA RM L9H17, 1949.
6. Rathert, George A., Jr., Rolls, L. Stewart, and Hanson, Carl M.: The Transonic Characteristics of a Low-Aspect-Ratio Triangular Wing With a Constant-Chord Flap as Determined by Wing-Flow Tests, Including Correlation With Large-Scale Tests. NACA RM A50E10, 1950.
7. Sandahl, Carl A., and Strass, H. Kurt: Comparative Tests of the Rolling Effectiveness of Constant-Chord, Full-Delta, and Half-Delta Ailerons on Delta Wings at Transonic and Supersonic Speeds. NACA RM L9J26, 1949.
8. Thomas, G. B.: Analysis of Supersonic Wind-Tunnel Tests of Balanced Aileron Configurations for the Nike Guided Missile. Douglas Aircraft Co. Rep. SM-13796, Sept. 1950.
9. Stone, David G.: Comparisons of the Effectiveness and Hinge Moments of All-Movable Delta and Flap-Type Controls on Various Wings. NACA RM L51C22, 1951.
10. Wiley, Harleth G.: Aerodynamic Characteristics at Transonic Speeds of a 60° Delta Wing Equipped With a Triangular Plan-Form Control Having a Skewed Hinge Axis and an Overhang Balance. Transonic Bump Method. NACA RM L50L01, 1951.
11. Martz, C. William, Church, James D., and Goslee, John W.: Free-Flight Investigation to Determine Force and Hinge-Moment Characteristics at Zero Angle of Attack of a 60° Swept-Back Half-Delta Tip Control on a 60° Swept-Back Delta Wing at Mach Numbers Between 0.68 and 1.44. NACA RM L51I14, 1951.
12. Strass, H. Kurt, and Marley, Edward T.: Rolling Effectiveness of All-Movable Wings at Small Angles of Incidence at Mach Numbers From 0.6 to 1.6. NACA RM L51H03, 1951.

13. Jaquet, Byron M., and Queijo, M. J.: Low-Speed Wind-Tunnel Investigation of Lateral Control Characteristics of a  $60^\circ$  Triangular-Wing Model Having Half-Delta Tip Controls. NACA RM L51110, 1951.
14. Niewald, Roy J., and Moul, Martin T.: The Longitudinal Stability, Control Effectiveness, and Control Hinge-Moment Characteristics Obtained from a Flight Investigation of a Canard Missile Configuration at Transonic and Supersonic Speeds. NACA RM L50I27, 1950.
15. Swanson, Robert S., and Toll, Thomas A.: Jet-Boundary Corrections for Reflection-Plane Models in Rectangular Wind Tunnels. NACA Rep. 770, 1943. (Formerly NACA ARR 3E22)

TABLE I.- COORDINATES FOR THE NACA 0005 (MODIFIED)<sup>1</sup> AIRFOIL SECTION  
[All dimensions in percent of wing chord]

Upper and lower surfaces

Station	Ordinate
0	0
1.25	.789
2.50	1.089
5.00	1.481
7.50	1.750
10.00	1.951
15.00	2.228
20.00	2.391
25.00	2.476
30.00	2.501
40.00	2.419
50.00	2.206
60.00	1.902
67.00	1.650
70.00	1.500
80.00	1.000
90.00	.500
100.00	0
L.E. radius: 0.275	T.E. radius: 0.05

<sup>1</sup>Straight lines aft of  
67-percent-chord station



TABLE II.- SUMMARY OF THE LIFT AND HINGE-MOMENT PARAMETERS FOR THE VARIOUS CONTROLS TESTED ON A TRIANGULAR WING OF ASPECT RATIO 2

Control	Percent balance	Flap-nose gap	Horn-balance contour	Trailing-edge thickness, (h/t)	$C_{L\alpha}$	$C_{L\delta}$	$C_{h\alpha}$	$C_{h\delta}$	Figure number
A	22.72	Unsealed	Normal	0	0.038	0.028	0	-0.0030	3(a),(b),(c), (d),(e),(f)
A	22.72	--do--	--do--	.5	.038	.027	-.0013	-.0034	10(a),(b),(c)
A	22.72	--do--	--do--	1.0	.038	.027	-.0017	-.0039	11(a),(b),(c)
B	16.98	--do--	--do--	0	.038	.027	-.0023	-.0043	4(a),(b),(c)
C	22.72	--do--	--do--	0	.038	.028	-.0018	-.0032	5(a),(b),(c)
C	22.72	Sealed	--do--	0	.038	.027	-.0018	-.0030	8(a),(b),(c)
C	22.72	--do--	Thin	0	.038	.027	-.0019	-.0036	9(a),(b),(c)
D	19.75	Unsealed	Normal	0	.038	.027	-.0027	-.0040	6(a),(b),(c)
E	16.98	--do--	--do--	0	.038	.027	-.0030	-.0043	7(a),(b),(c)



CONFIDENTIAL  
SECURITY INFORMATION

CONFIDENTIAL  
SECURITY INFORMATION

NACA RM A52F13

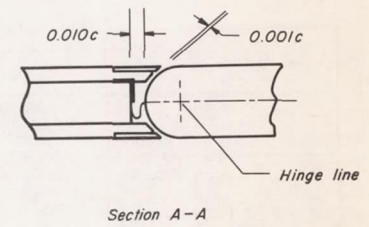
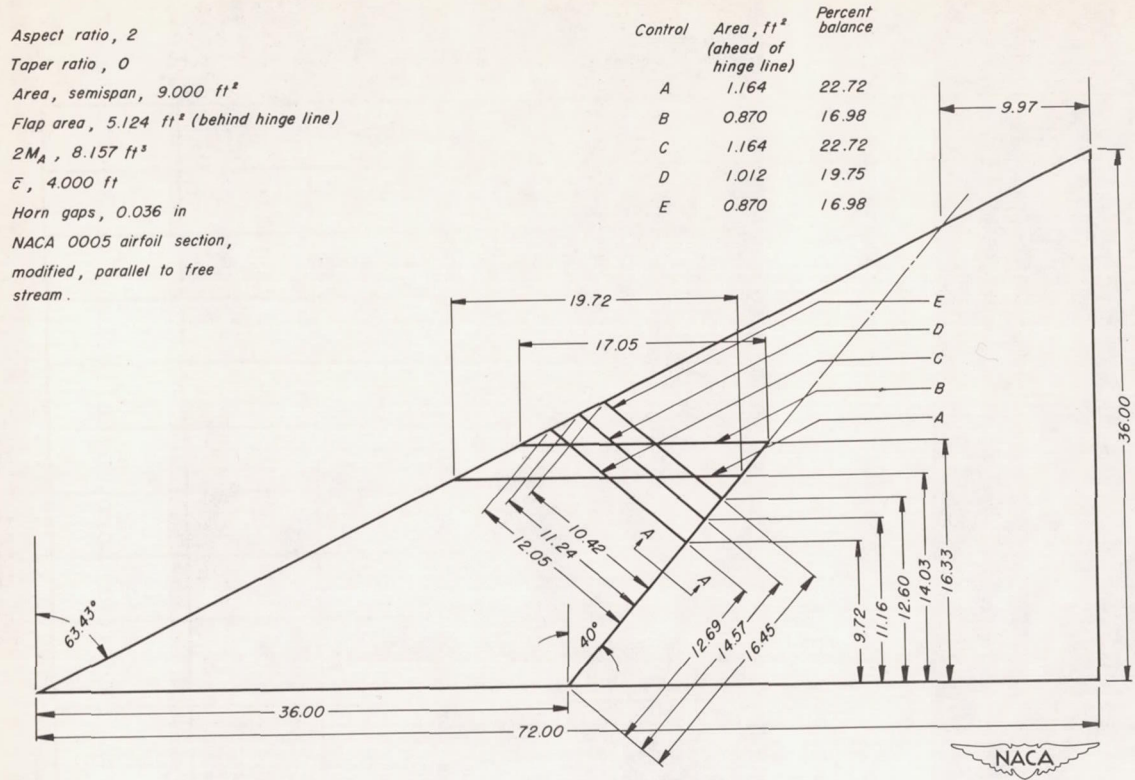
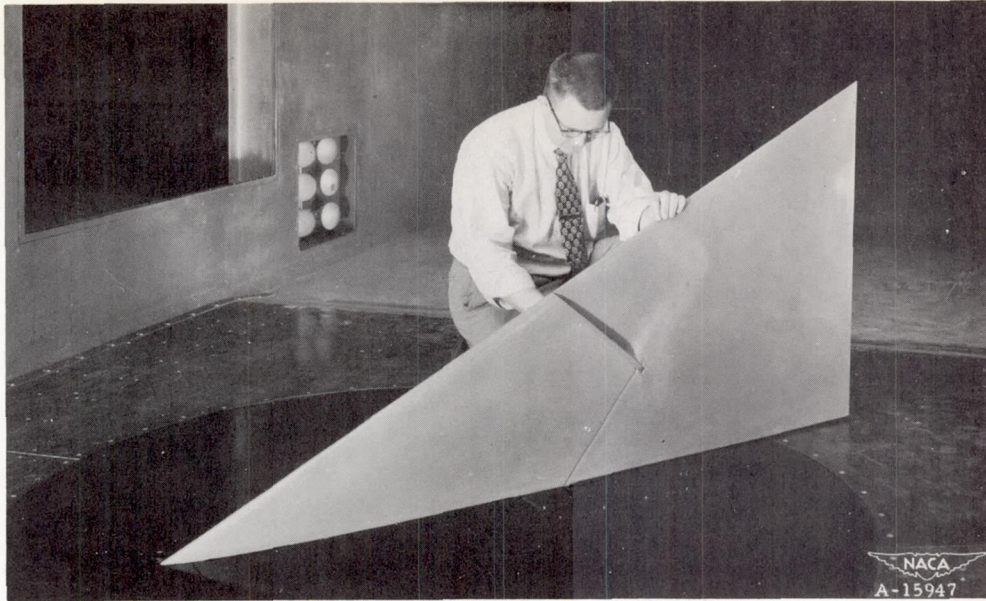
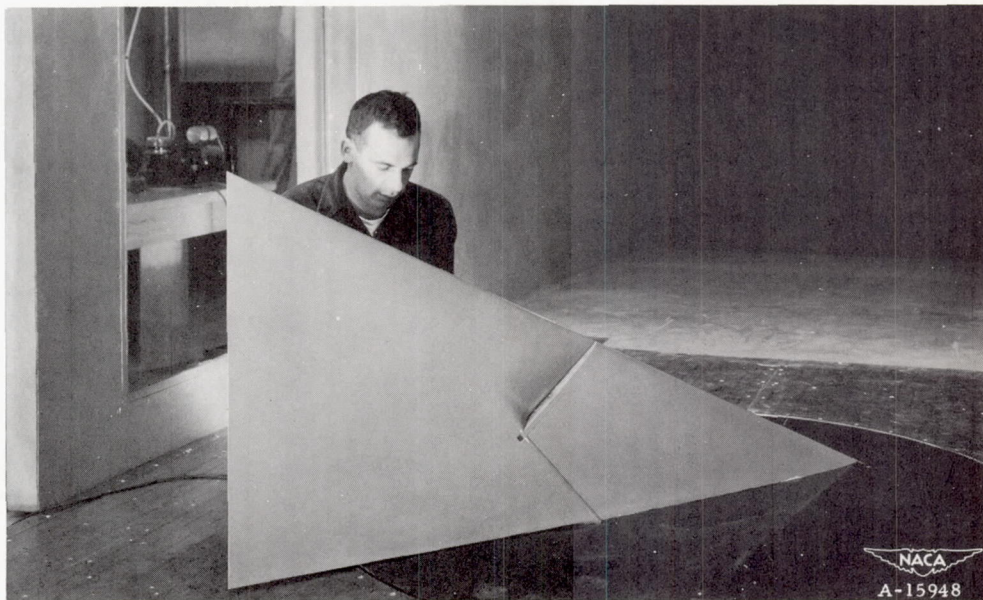


Figure 1.- Geometry of the model showing the controls tested.

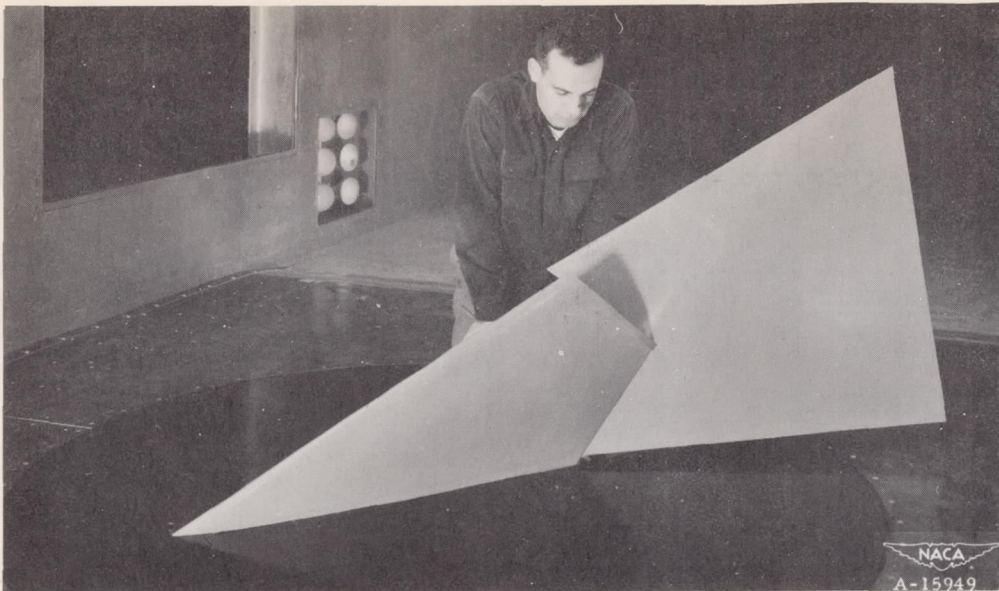


(a) Control C, thin contour horn, undeflected, three-quarter front view.

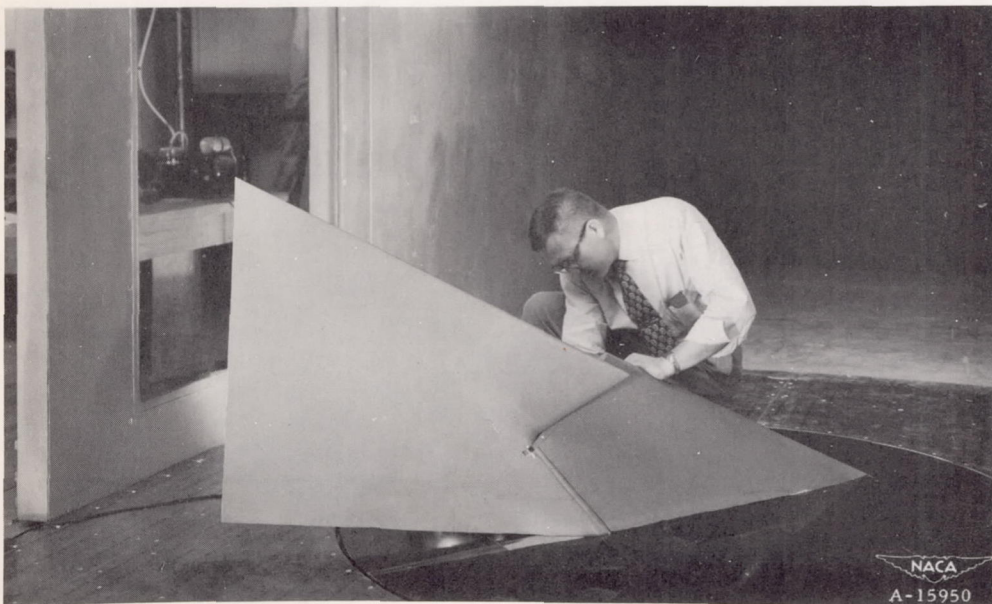


(b) Control C, thin contour horn, undeflected, three-quarter rear view.

Figure 2.- Triangular wing of aspect ratio 2 having a large-chord horn-balanced flap-type control.

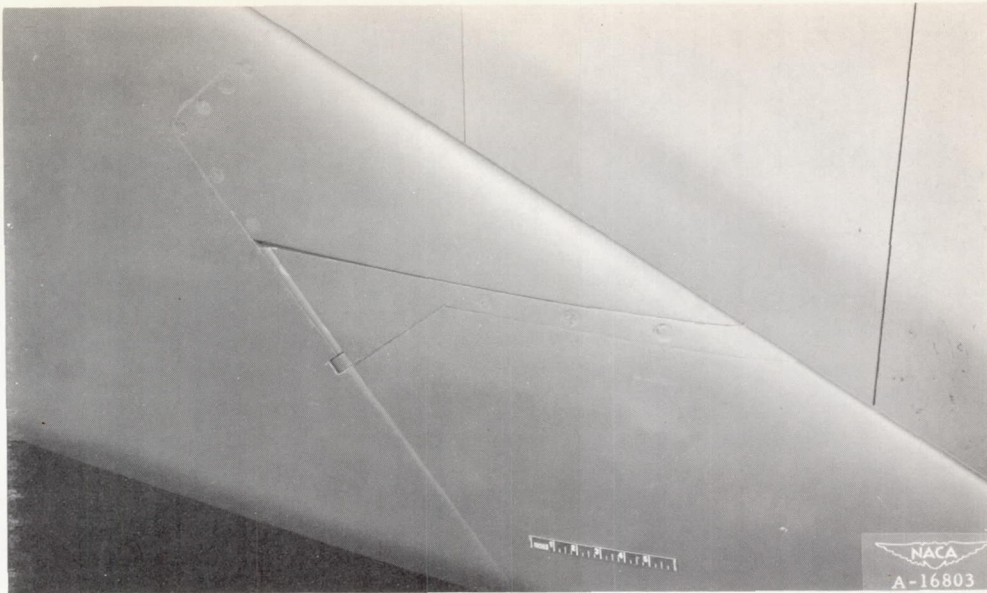


(c) Control C, thin contour horn, flap deflected  $-30^{\circ}$ , three-quarter front view.

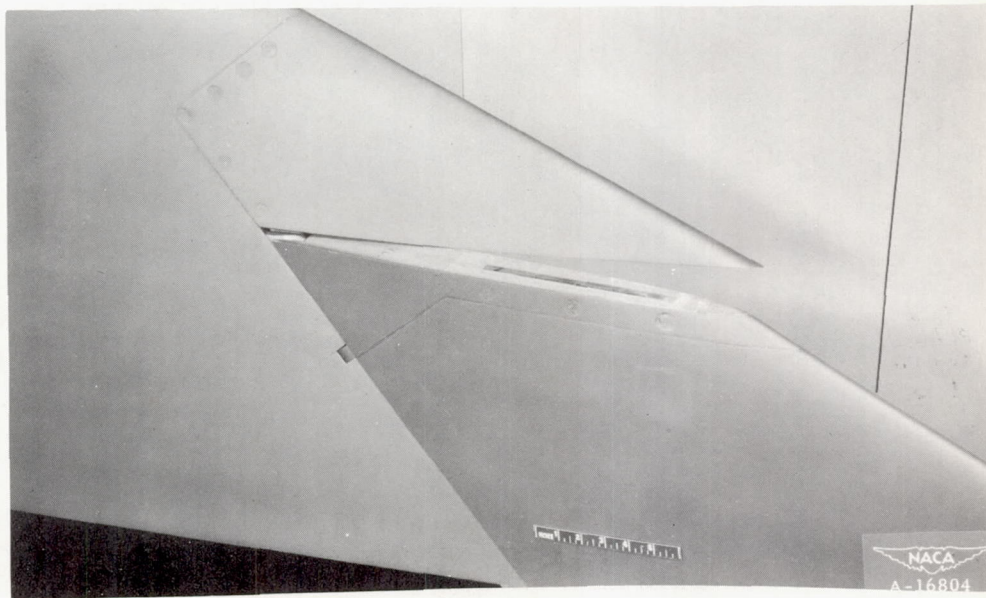


(d) Control C, thin contour horn, flap deflected  $-30^{\circ}$ , three-quarter rear view.

Figure 2.- Continued.

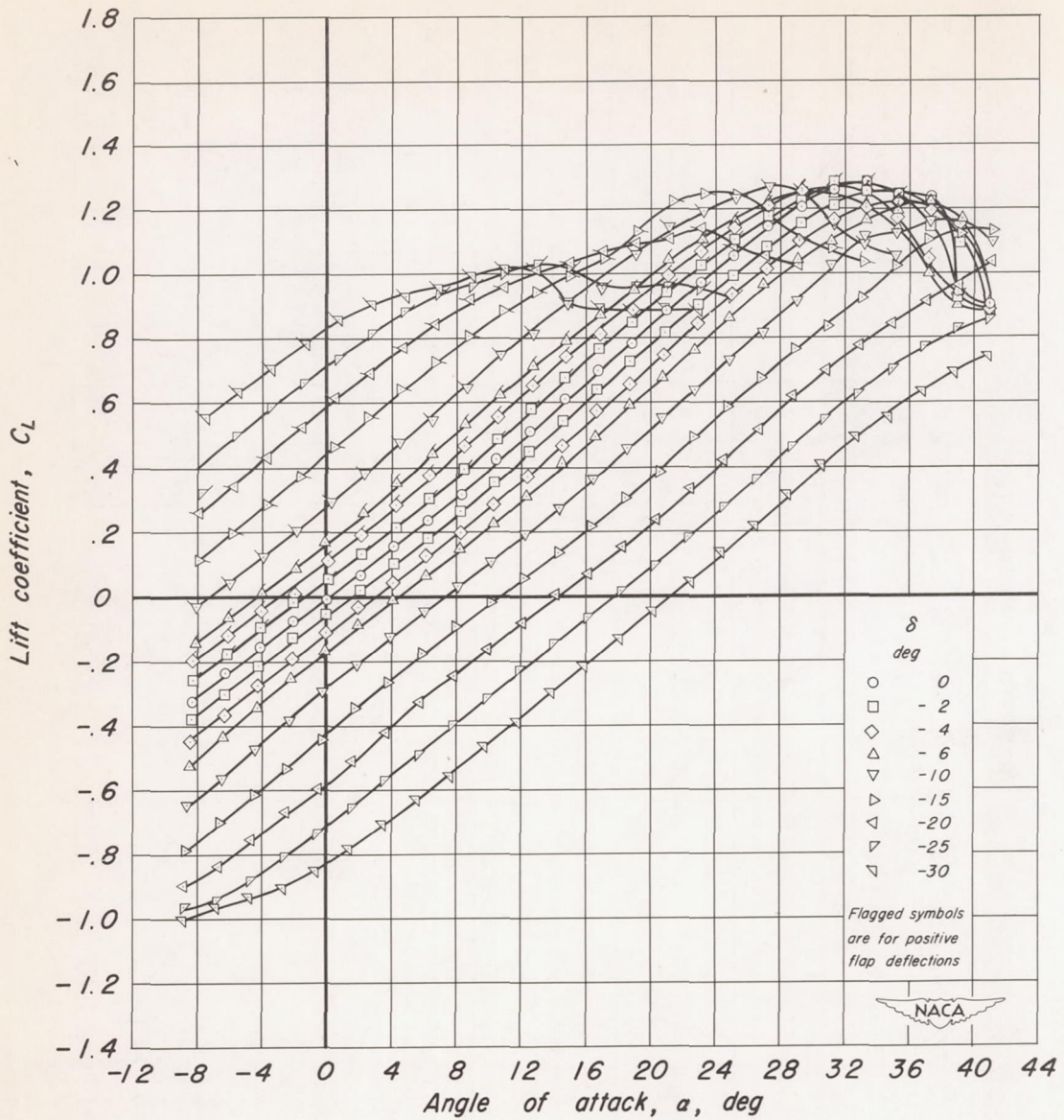


(e) Control A, normal contour horn, flap undeflected, three-quarter front view.



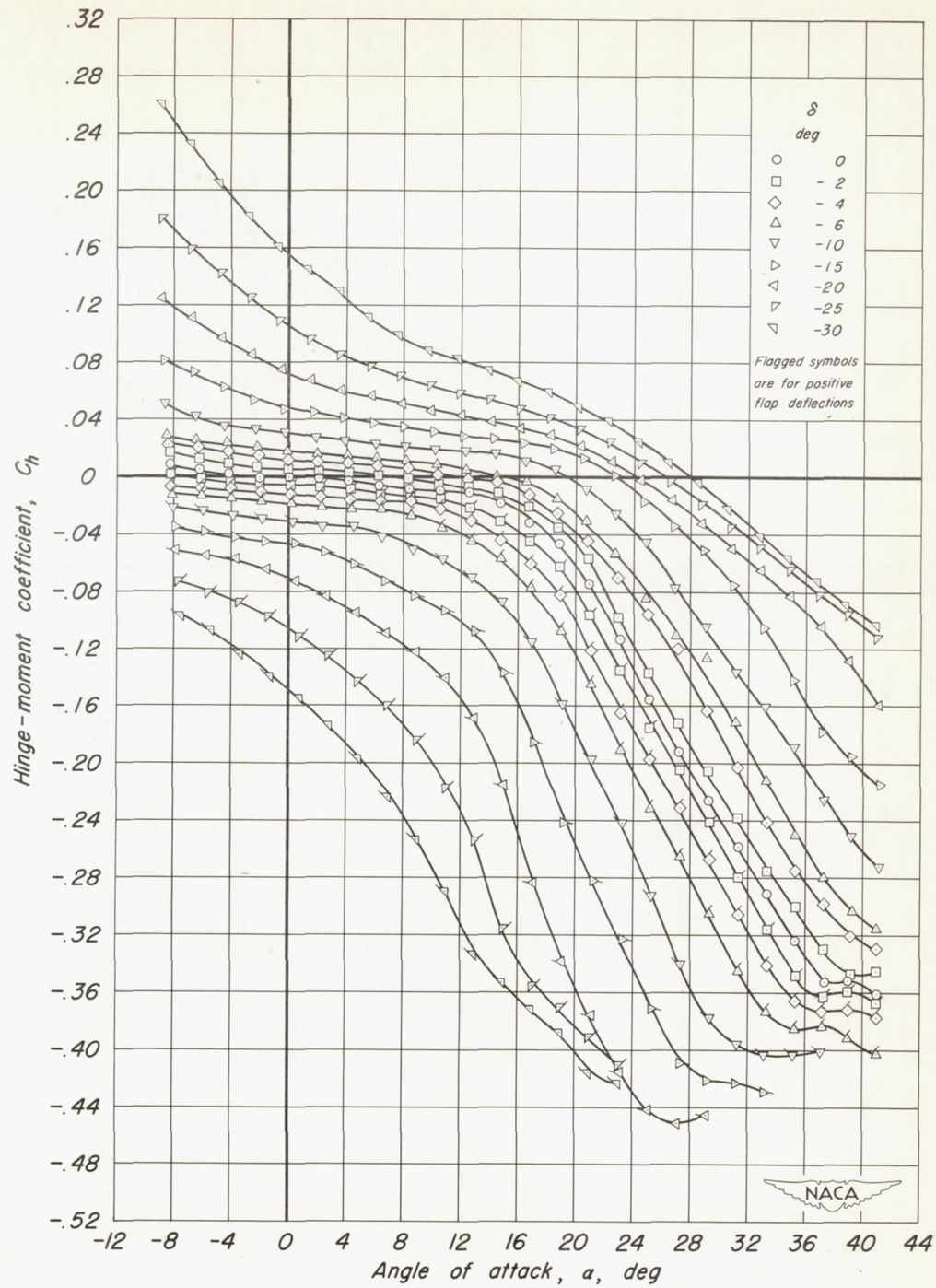
(f) Control A, normal contour horn, flap deflected  $-30^{\circ}$ , three-quarter front view.

Figure 2.- Concluded.



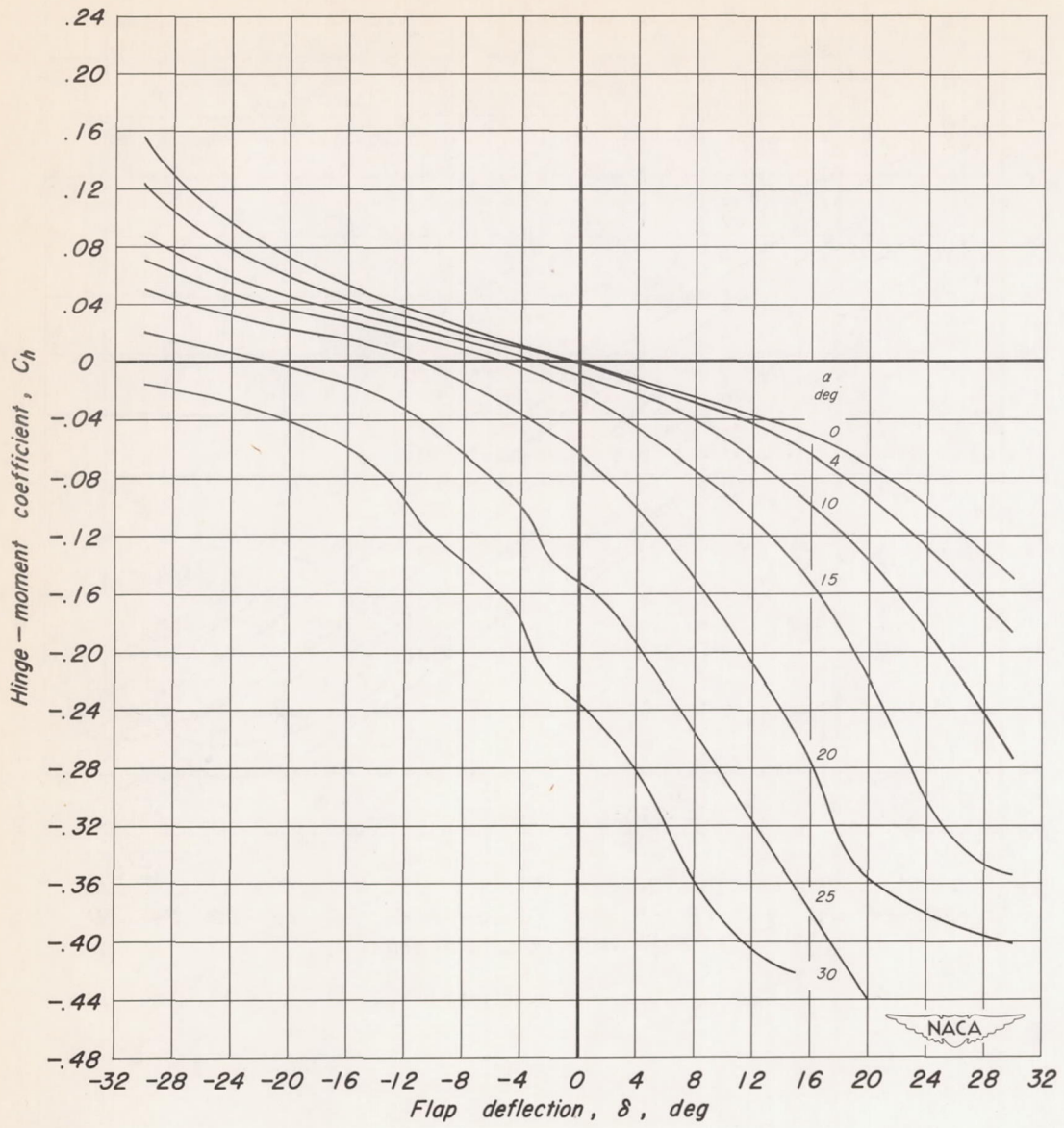
(a)  $C_L$  vs  $a$

Figure 3.— Lift and hinge-moment characteristics of horn-balanced control A on a triangular wing; 22.72 percent balance, normal contour horn, unsealed, trailing-edge thickness,  $h/t = 0$ .



(b)  $C_h$  vs  $a$

Figure 3.-Continued.



(c)  $C_h$  vs  $\delta$

Figure 3.- Continued.

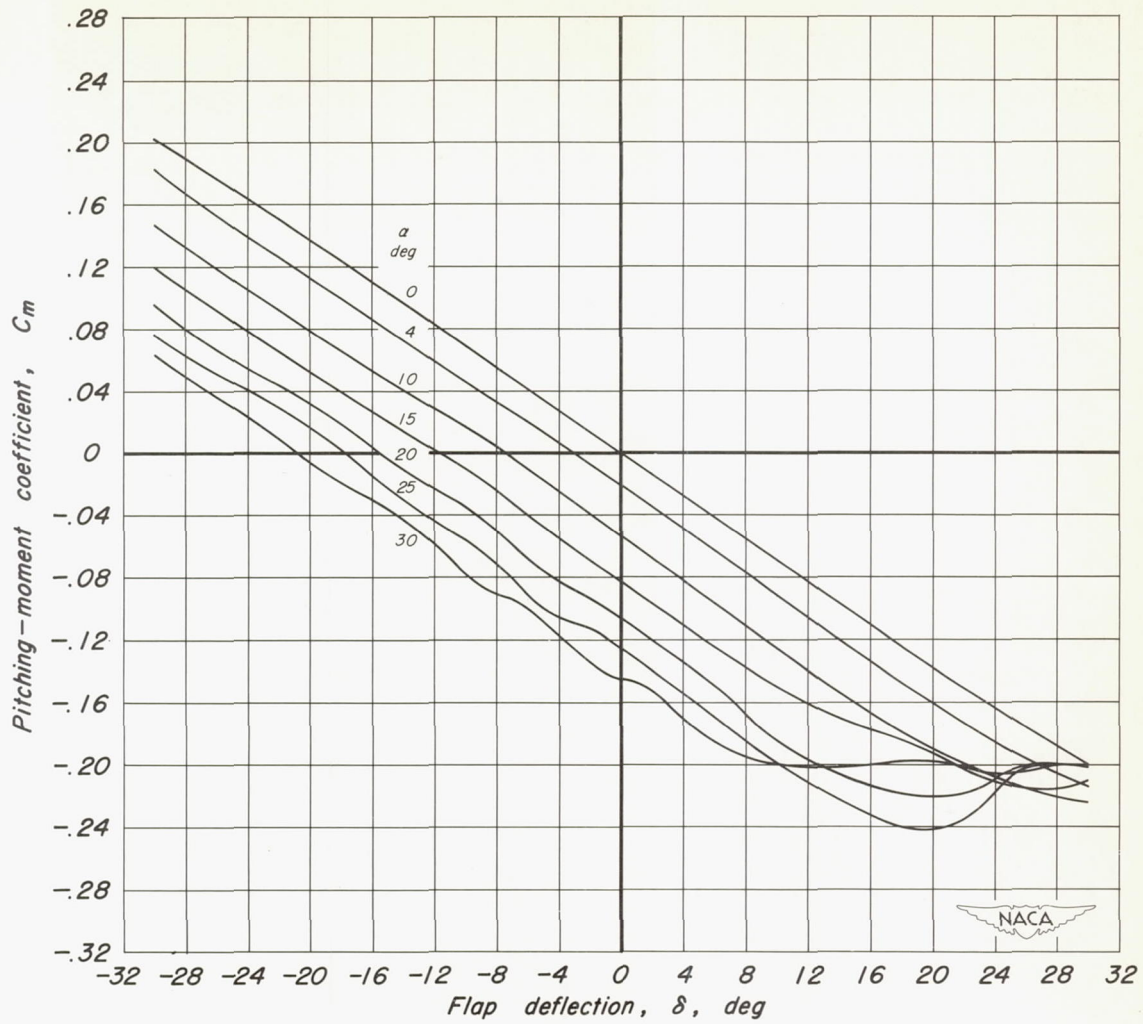
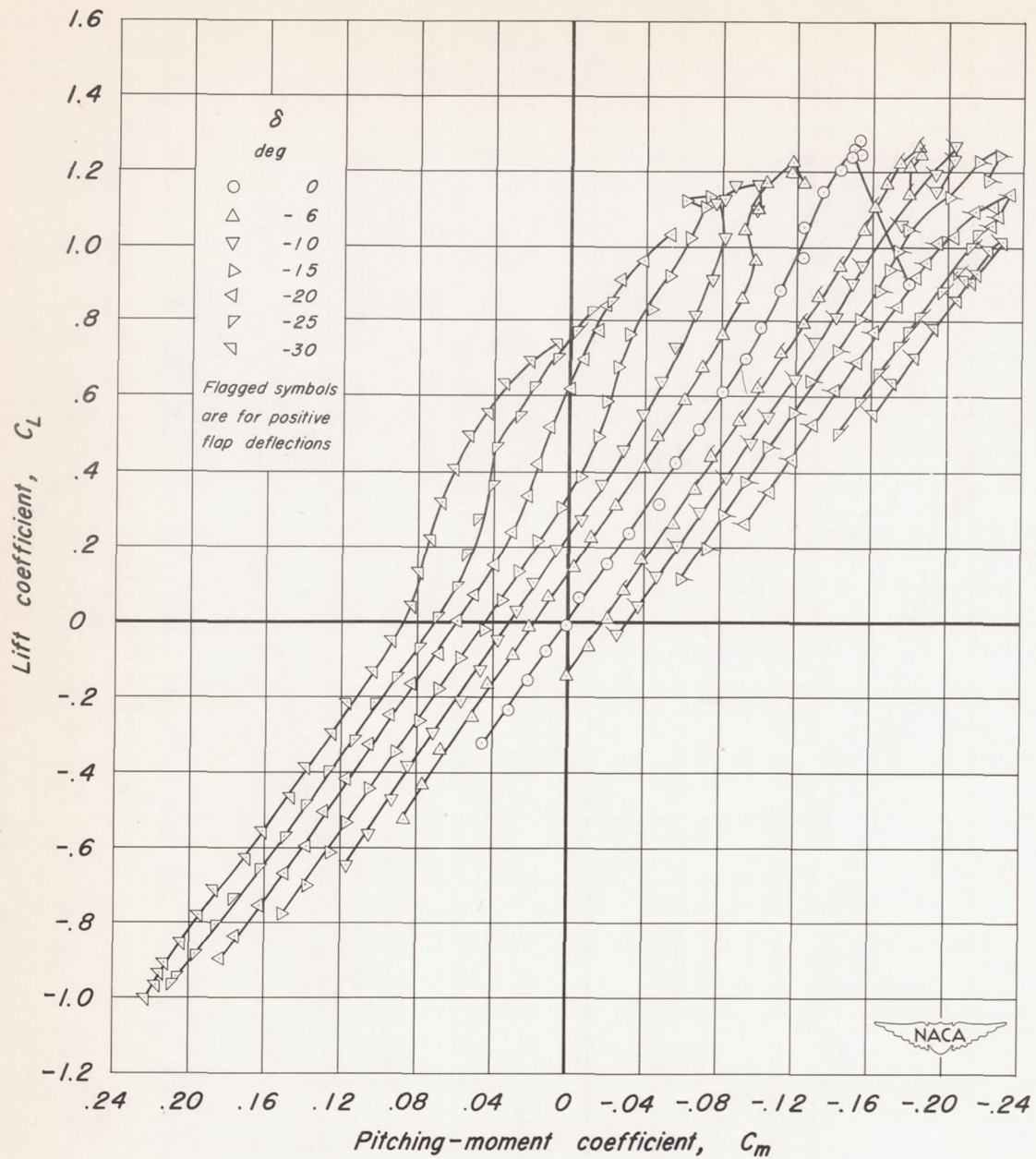
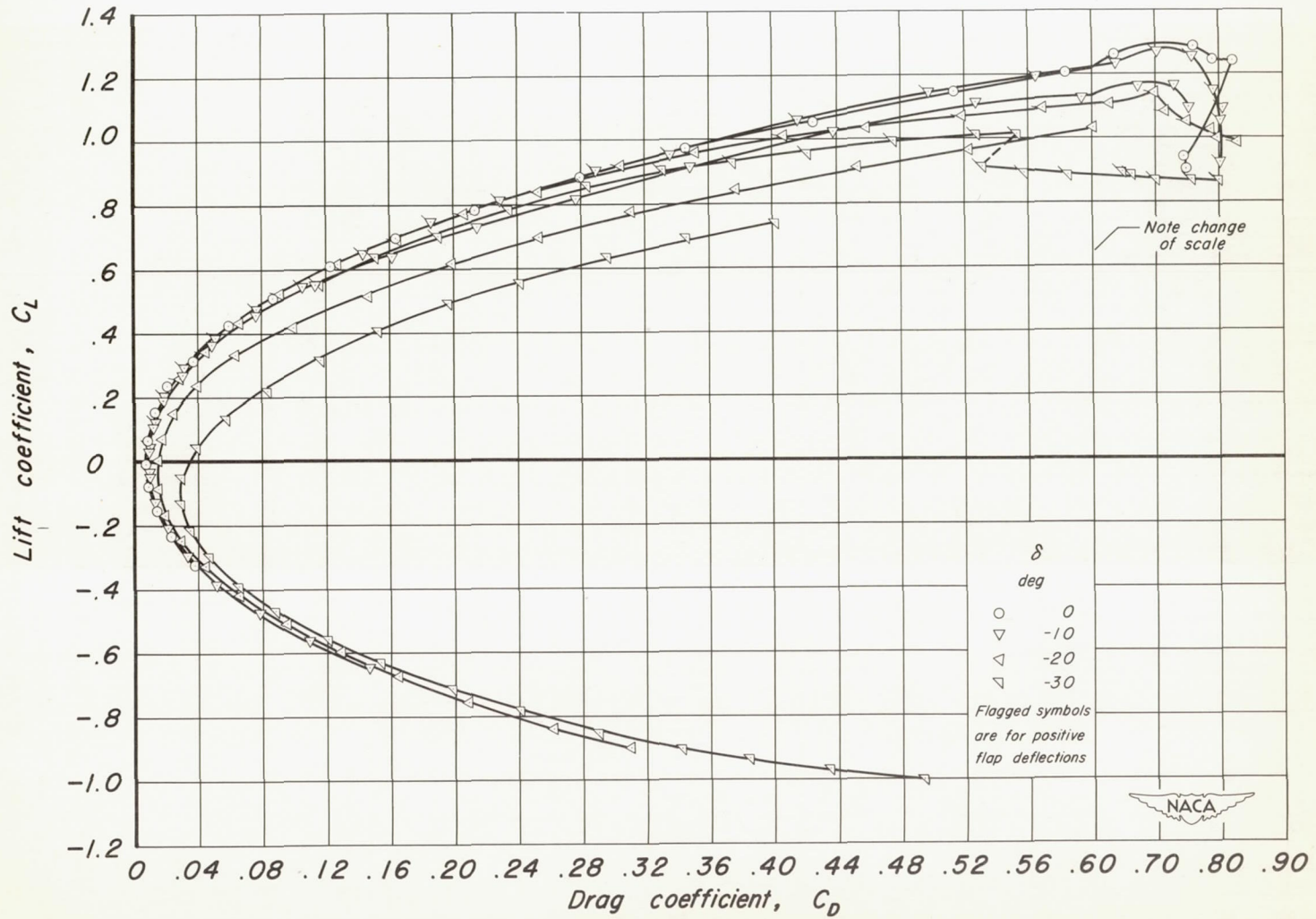
(d)  $C_m$  vs  $\delta$ 

Figure 3.- Continued.



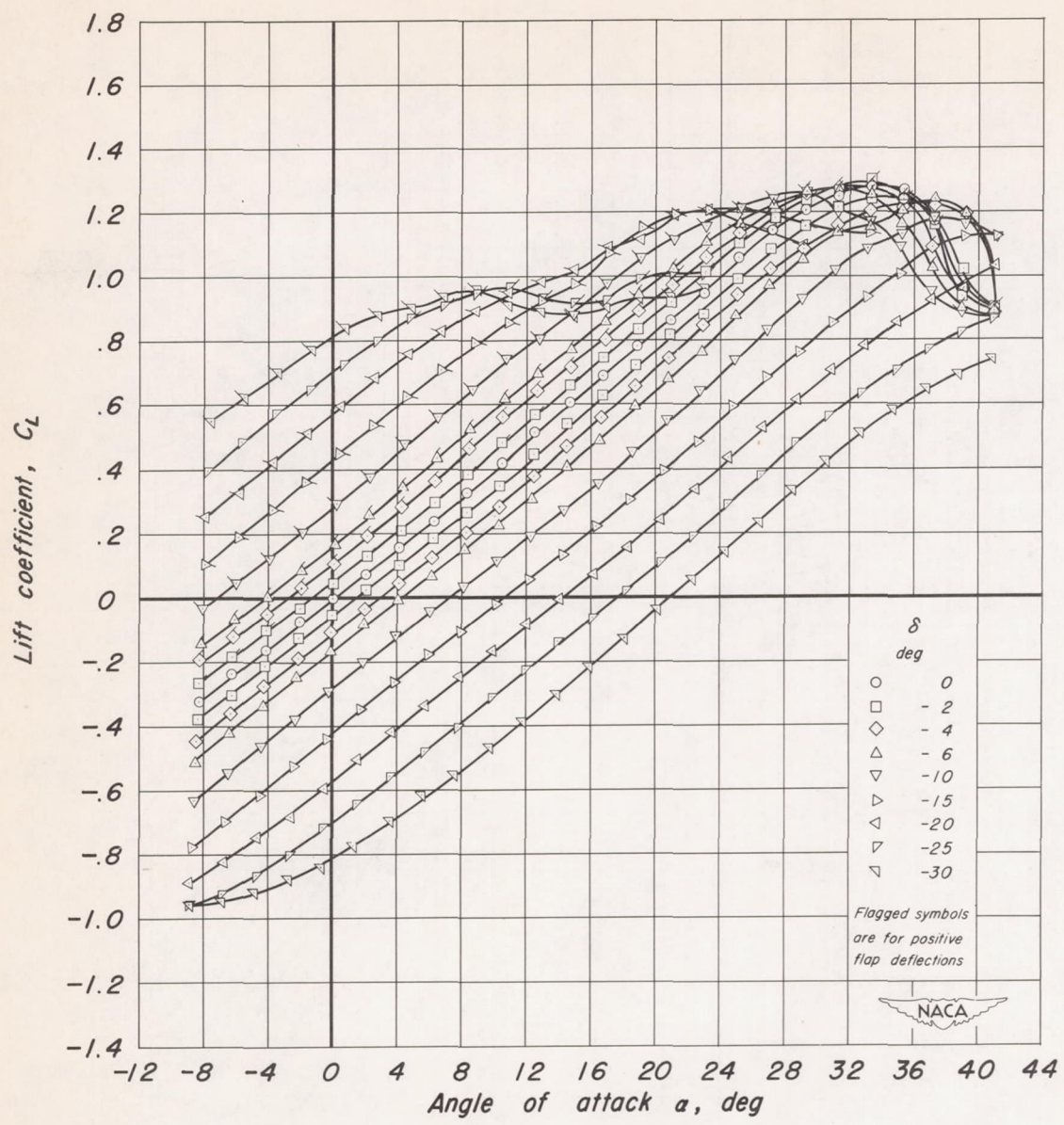
(e)  $C_m$  vs  $C_L$

Figure 3.-Continued.



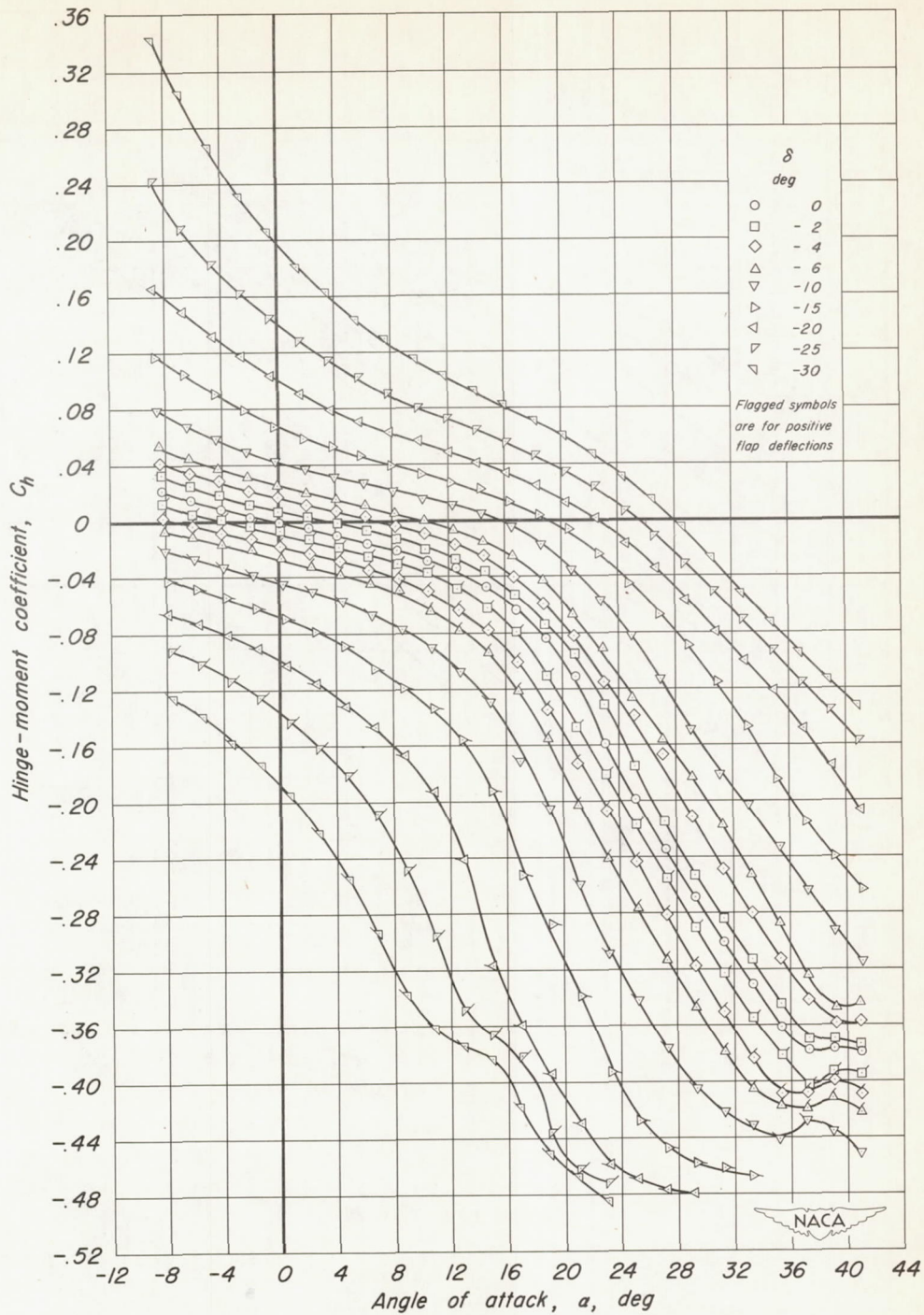
(f)  $C_L$  vs  $C_D$

Figure 3.- Concluded.



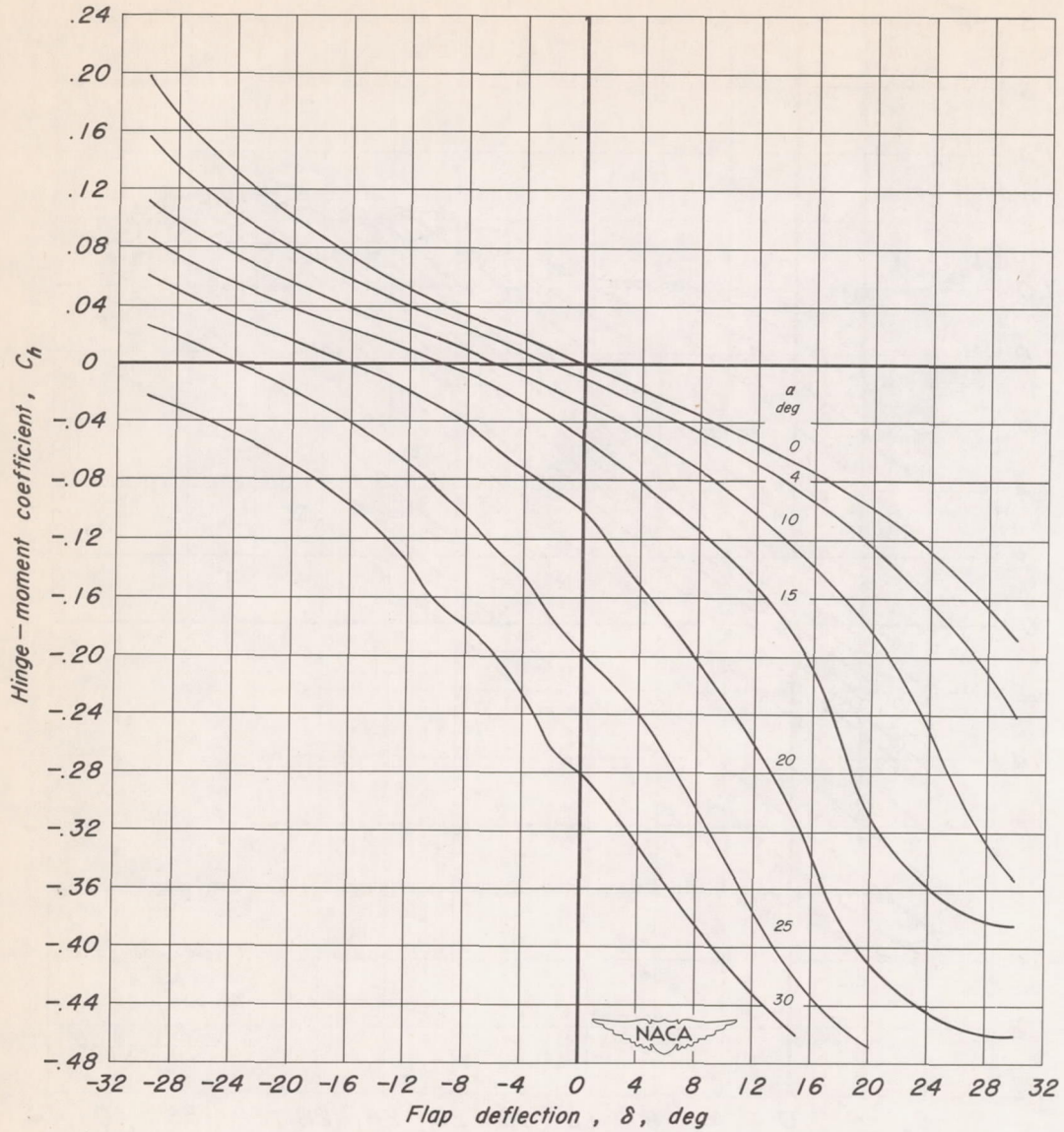
(a)  $C_L$  vs  $a$

Figure 4.—Lift and hinge-moment characteristics of horn-balanced control B on a triangular wing; 16.98 percent balance, normal contour horn, unsealed, trailing-edge thickness,  $h/t = 0$ .



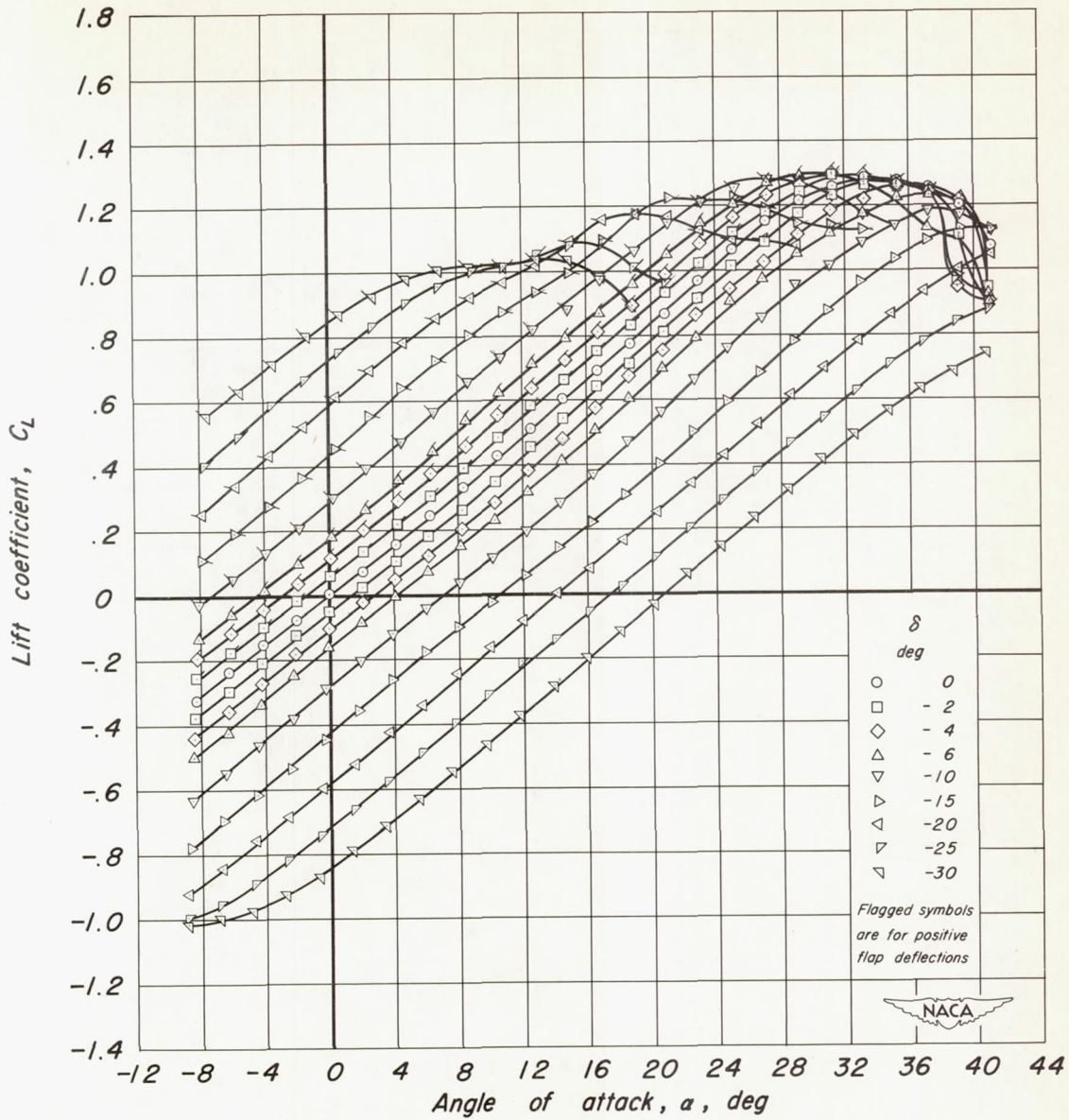
(b)  $C_h$  vs  $a$

Figure 4.- Continued.



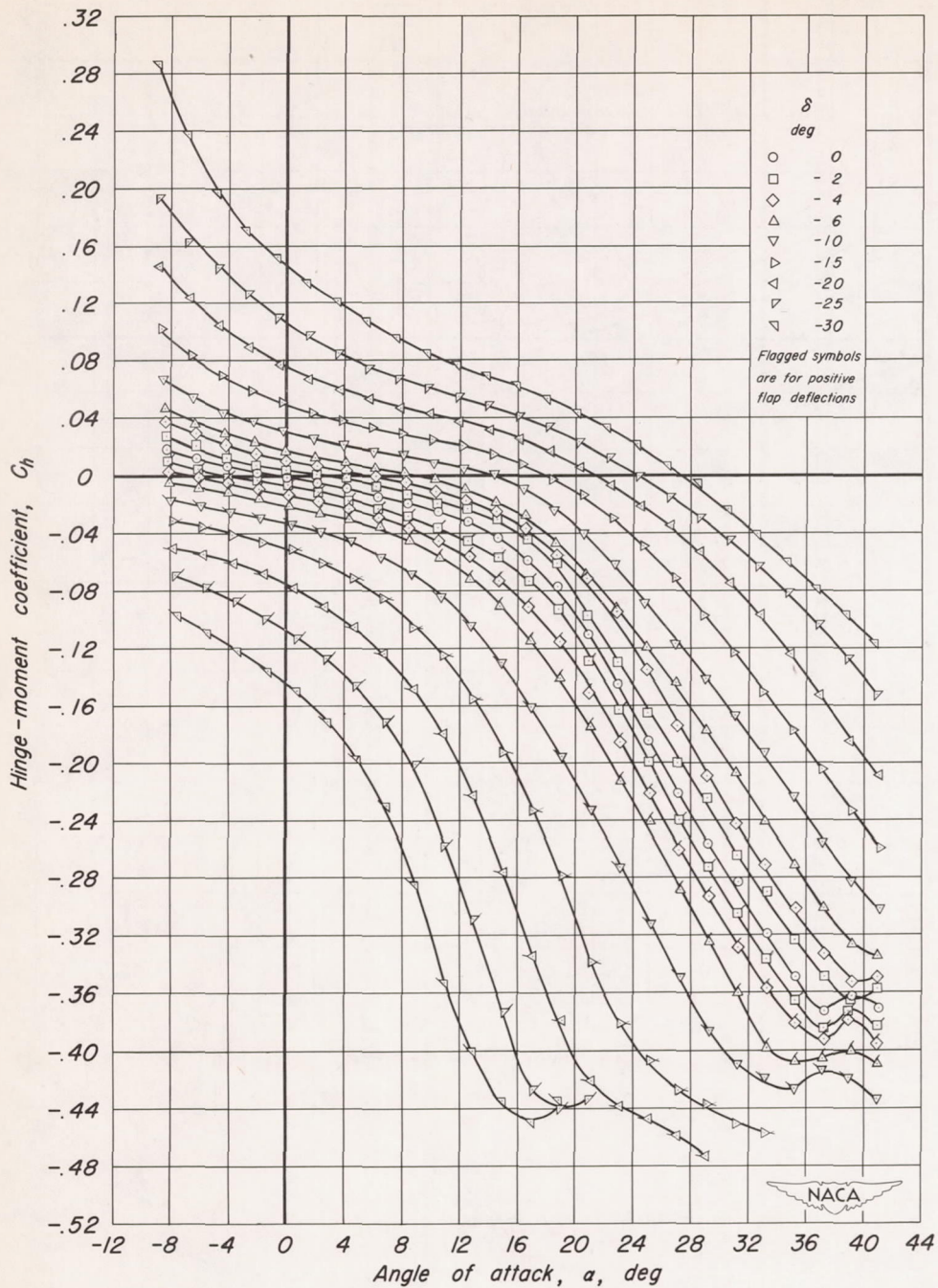
(c)  $C_h$  vs  $\delta$

Figure 4.- Concluded.



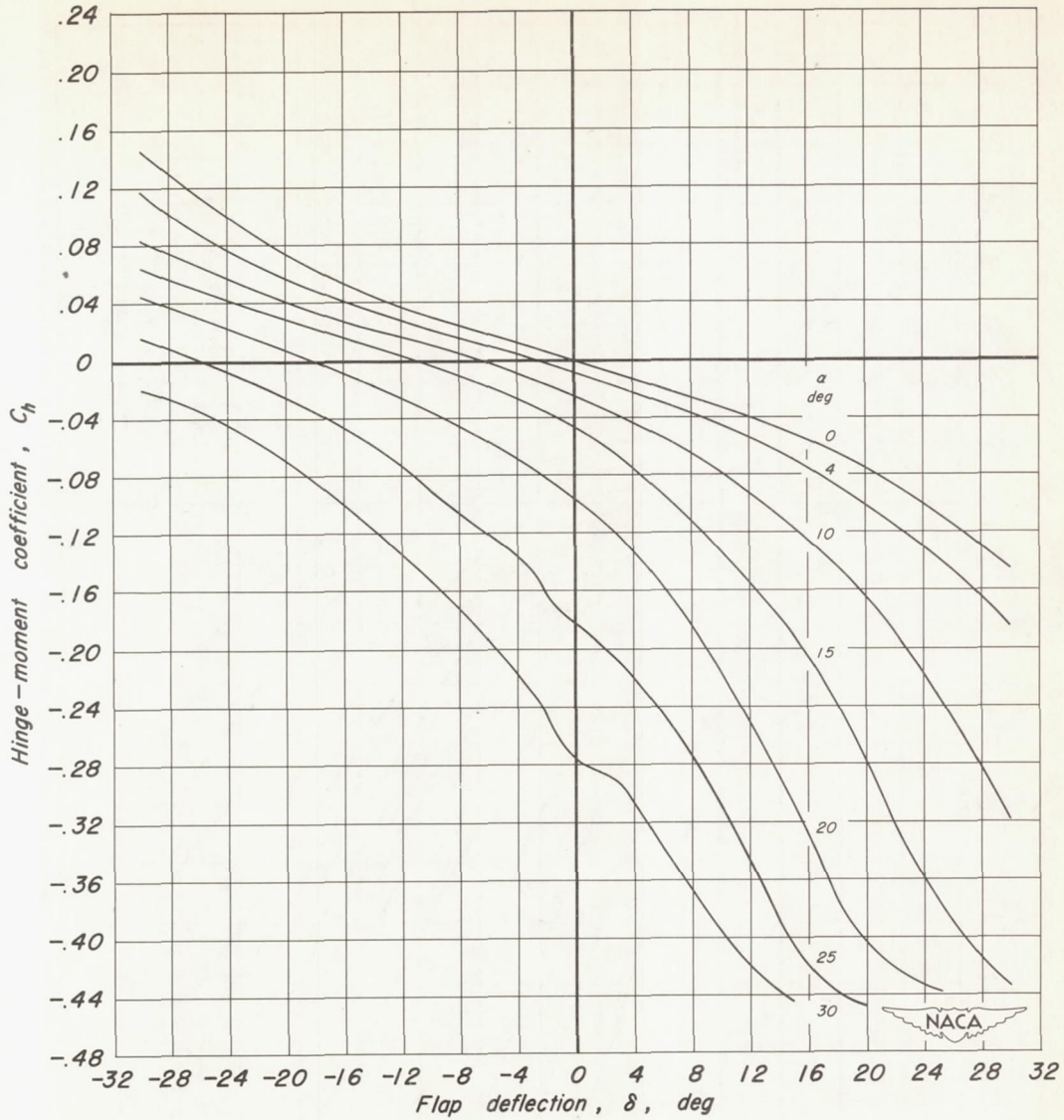
(a)  $C_L$  vs  $\alpha$

Figure 5.— Lift and hinge-moment characteristics of horn-balanced control C on a triangular wing; 22.72 percent balance, normal contour horn, unsealed, trailing-edge thickness,  $h/t = 0$ .



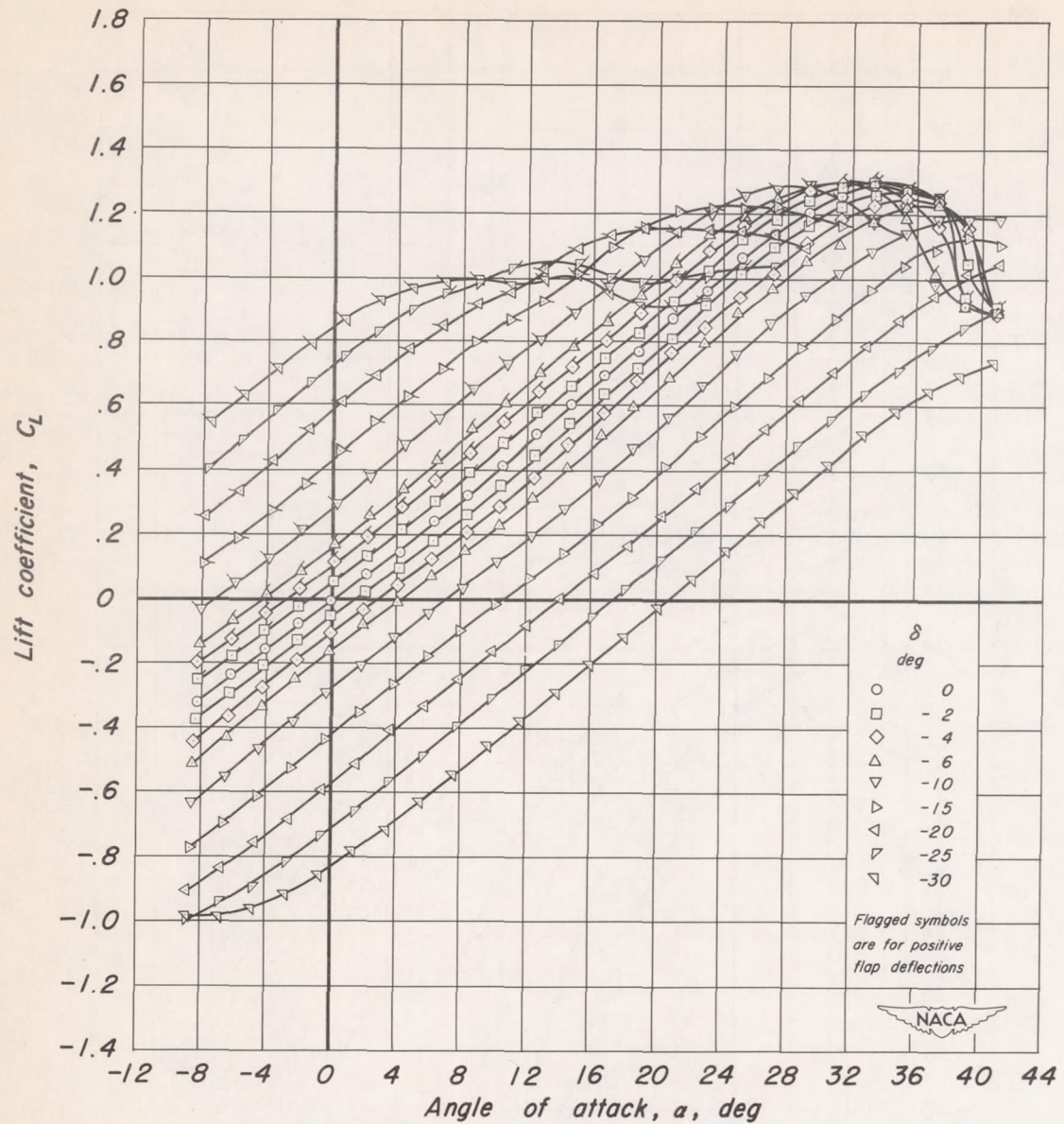
(b)  $C_h$  vs  $a$

Figure 5.- Continued.



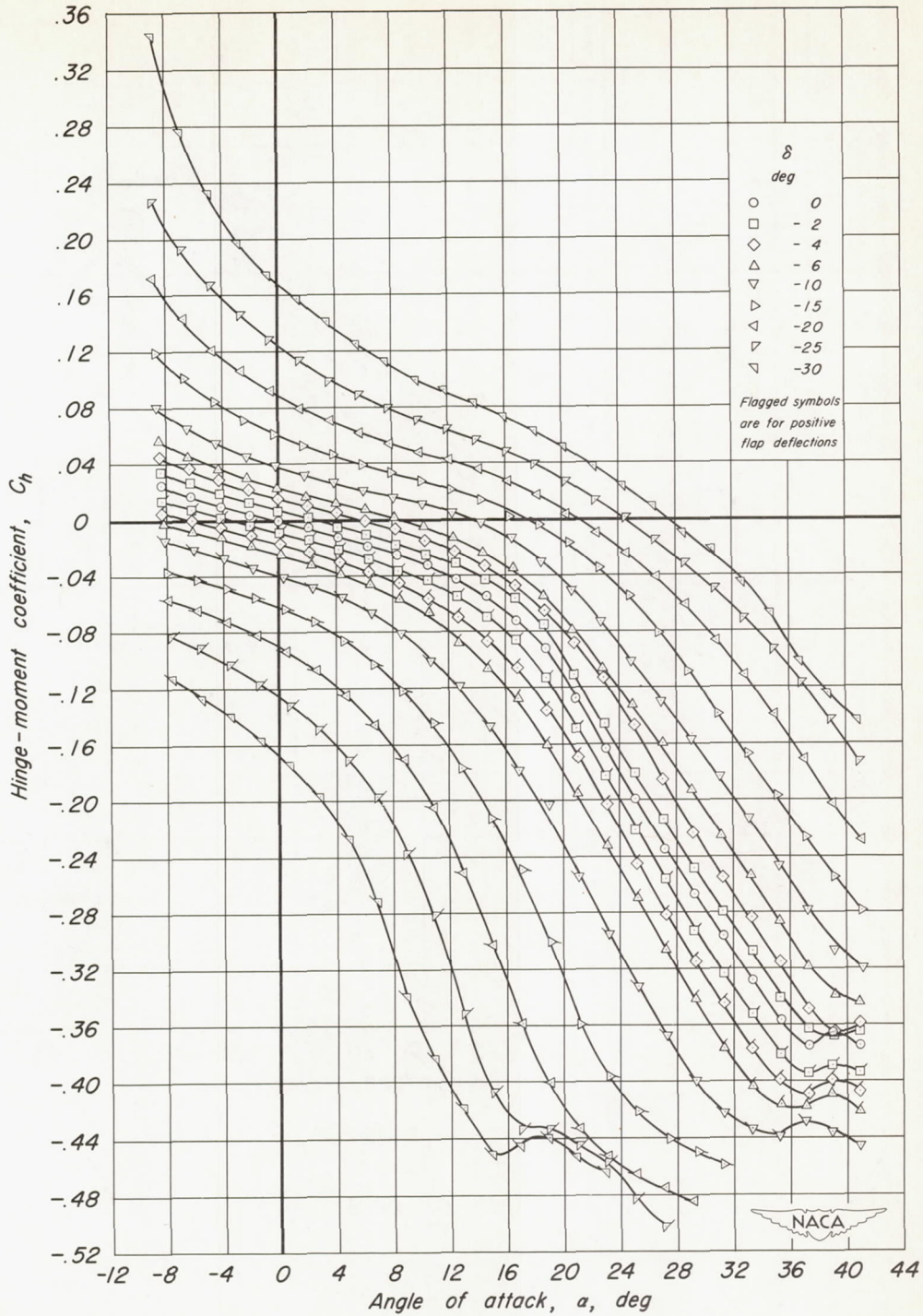
(c)  $C_h$  vs  $\delta$

Figure 5.-Concluded.



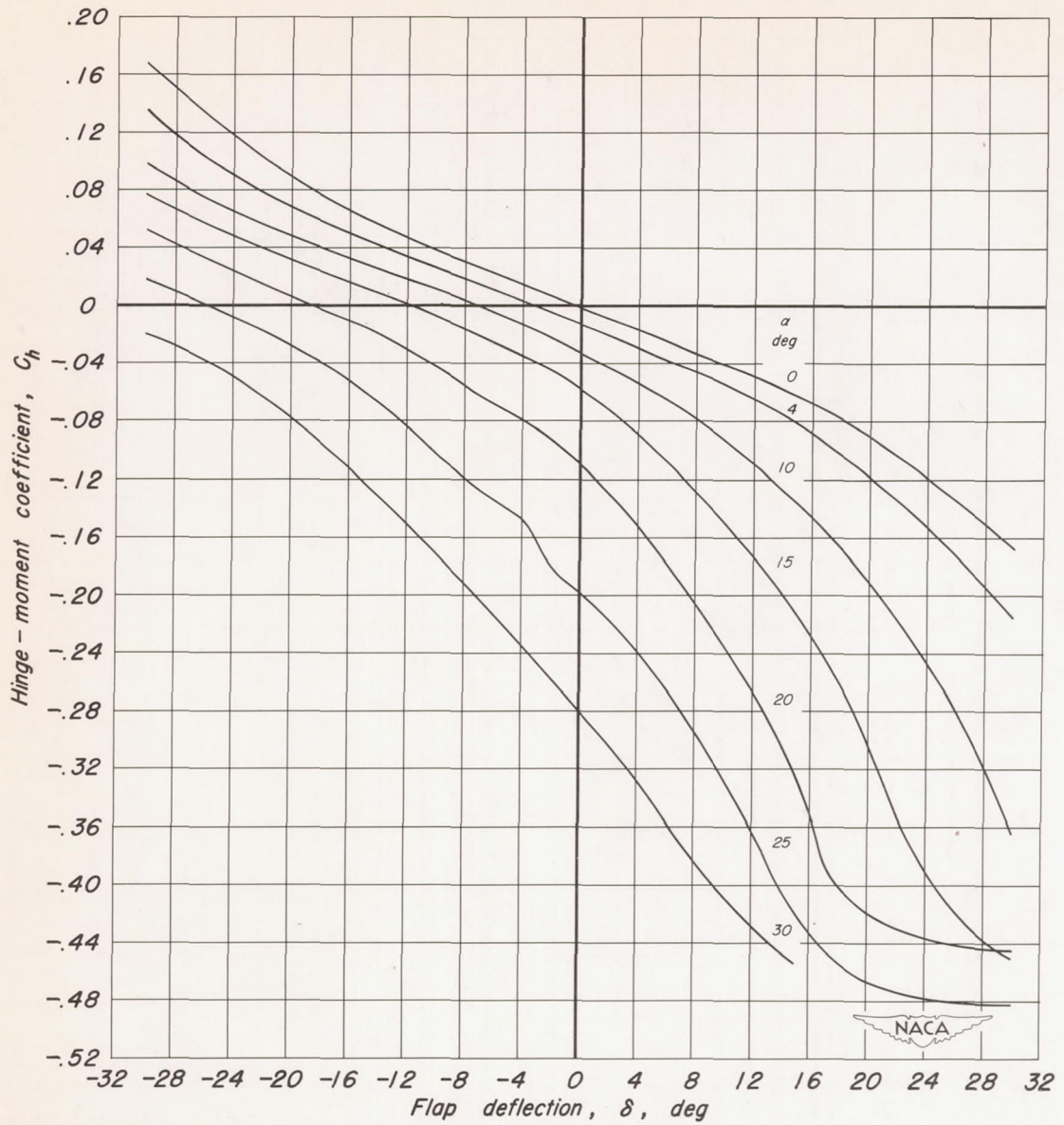
(a)  $C_L$  vs  $a$

Figure 6.- Lift and hinge-moment characteristics of horn-balanced control D on a triangular wing; 19.75 percent balance, normal contour horn, unsealed, trailing-edge thickness,  $h/t = 0$ .



(b)  $C_h$  vs  $a$

Figure 6.—Continued.



(c)  $C_h$  vs  $\delta$

Figure 6.- Concluded.

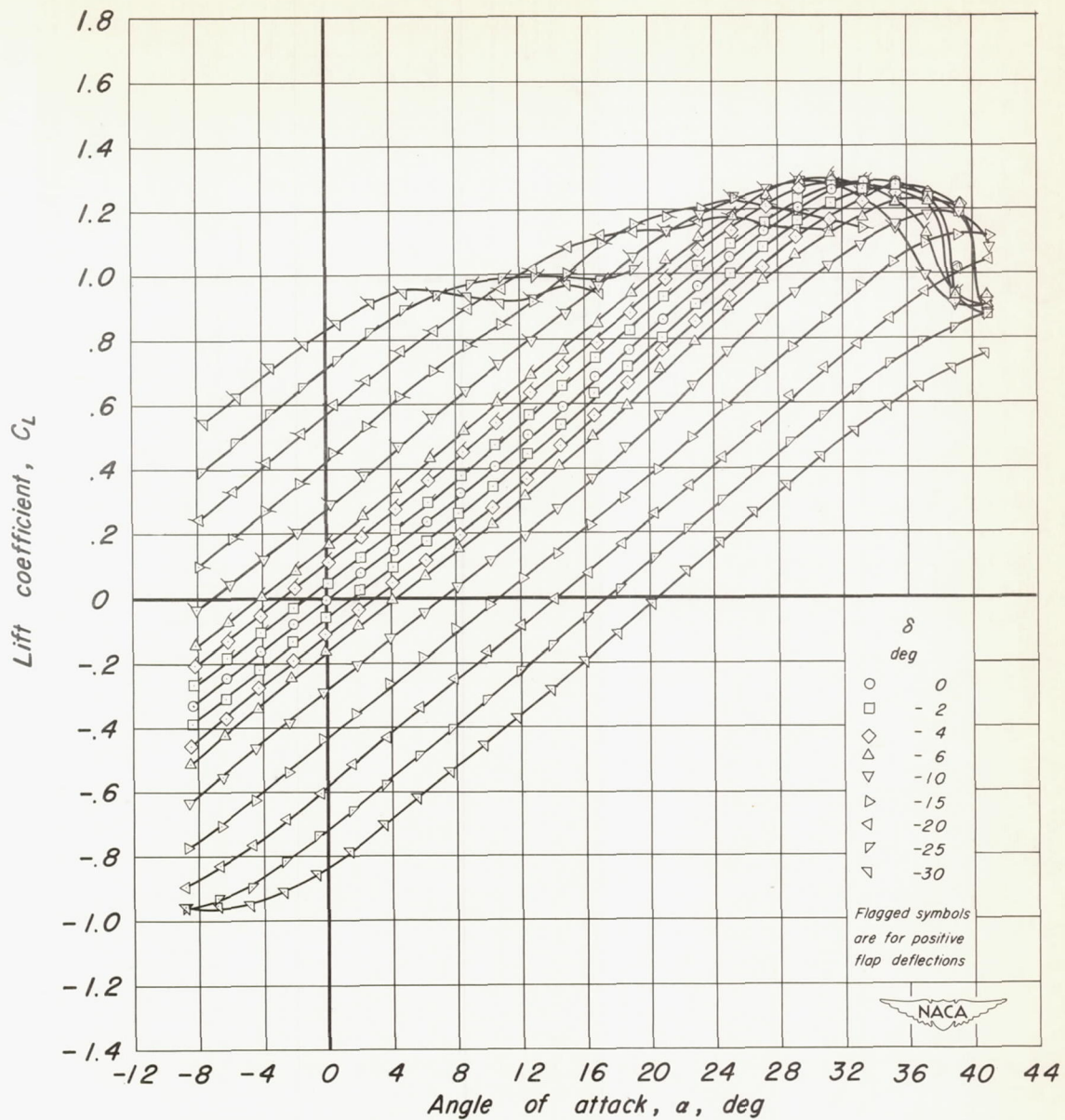
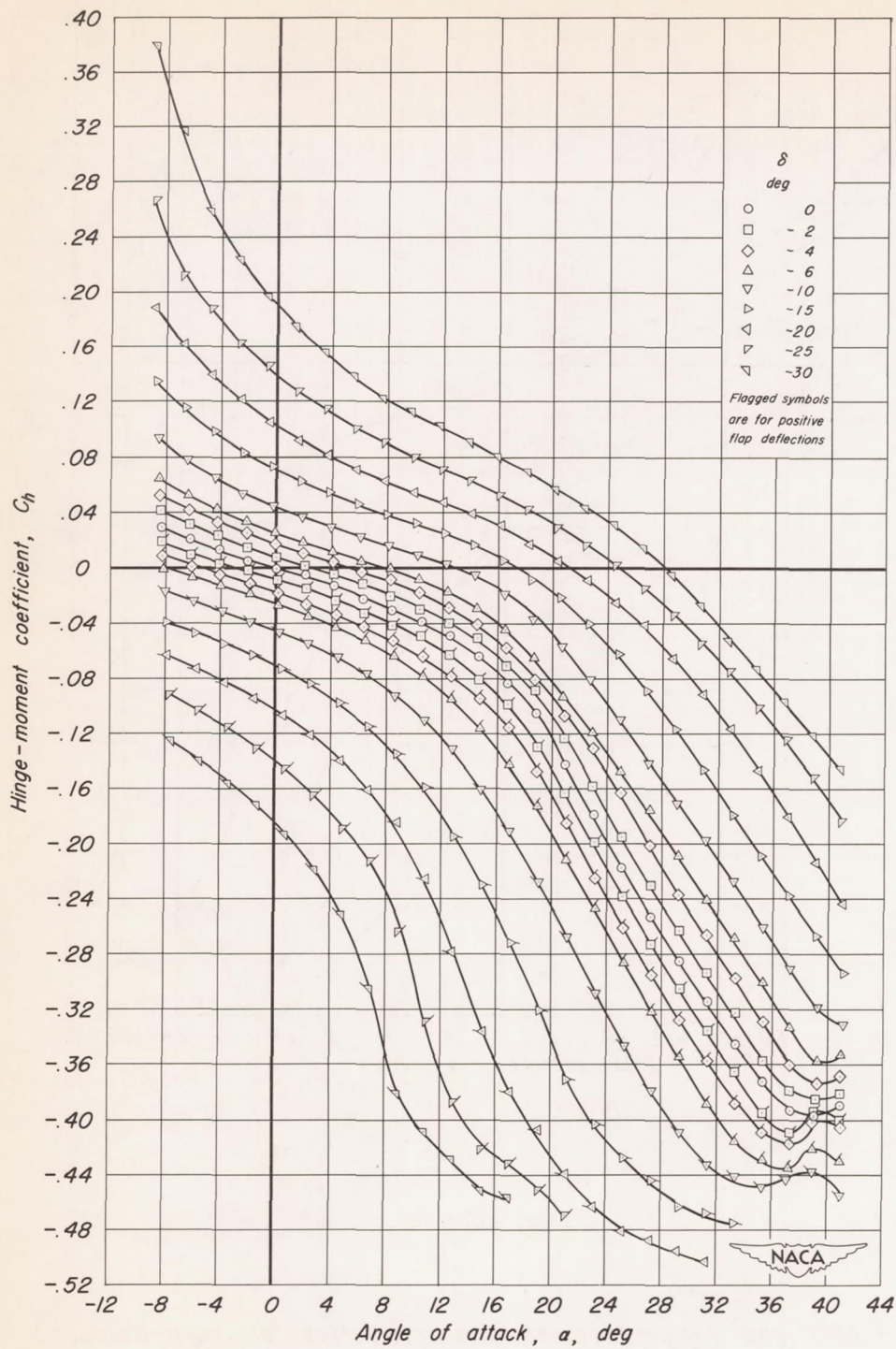
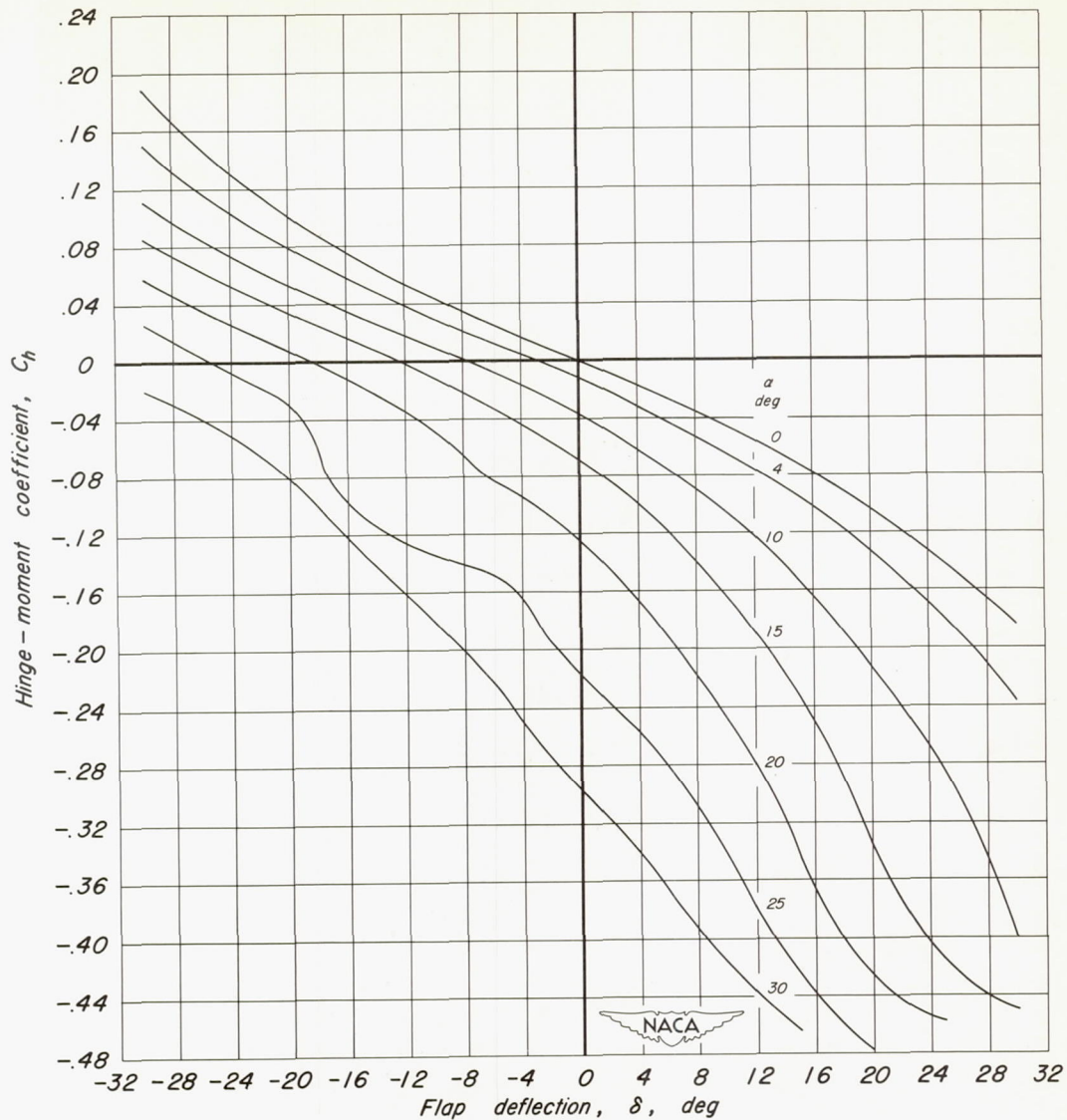
(a)  $C_L$  vs  $\alpha$ 

Figure 7.— Lift and hinge-moment characteristics of horn-balanced control E on a triangular wing; 16.98 percent balance, normal contour horn, unsealed, trailing-edge thickness,  $h/t = 0$ .

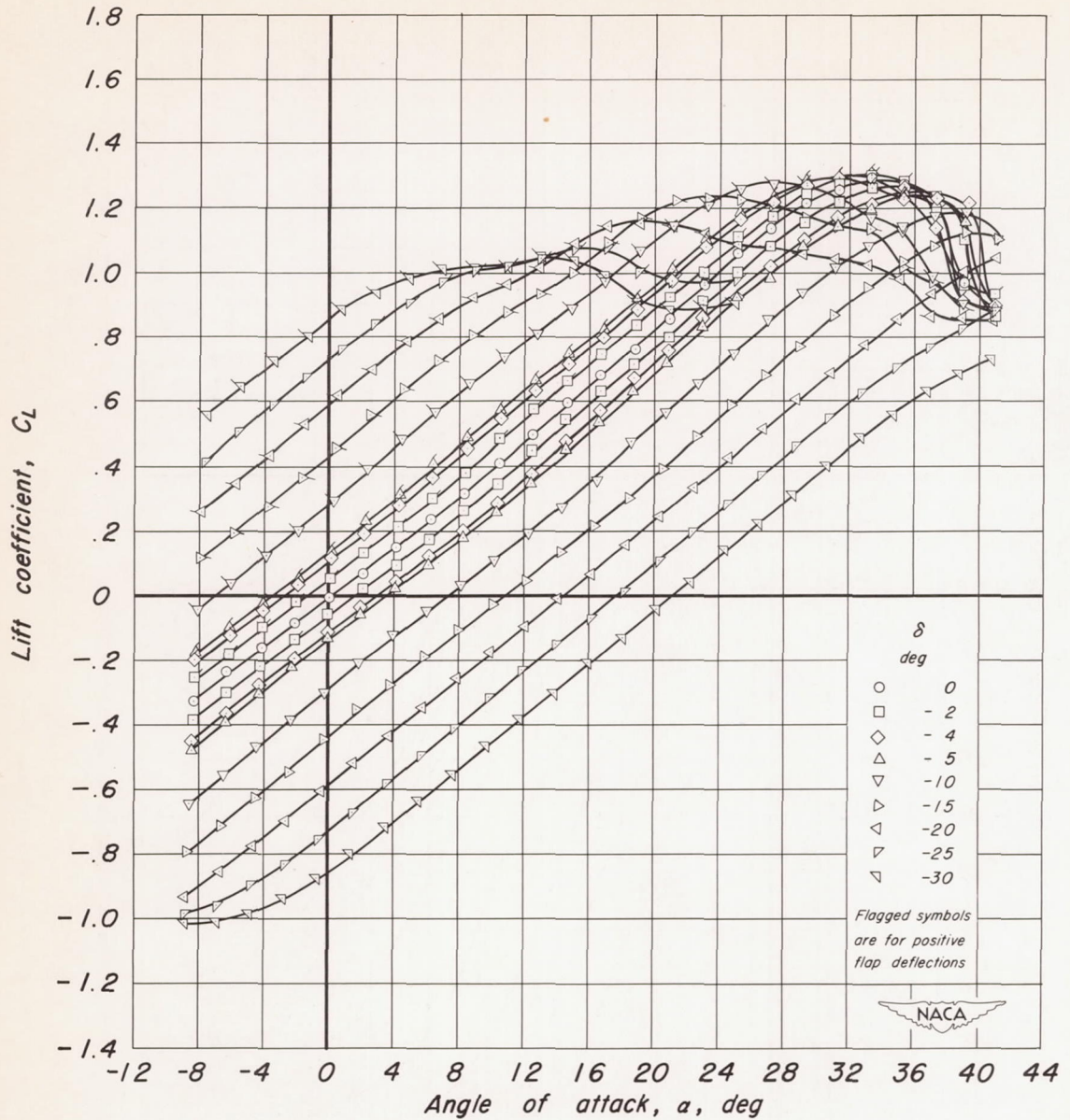


(b)  $C_h$  vs  $a$   
Figure 7.— Continued.



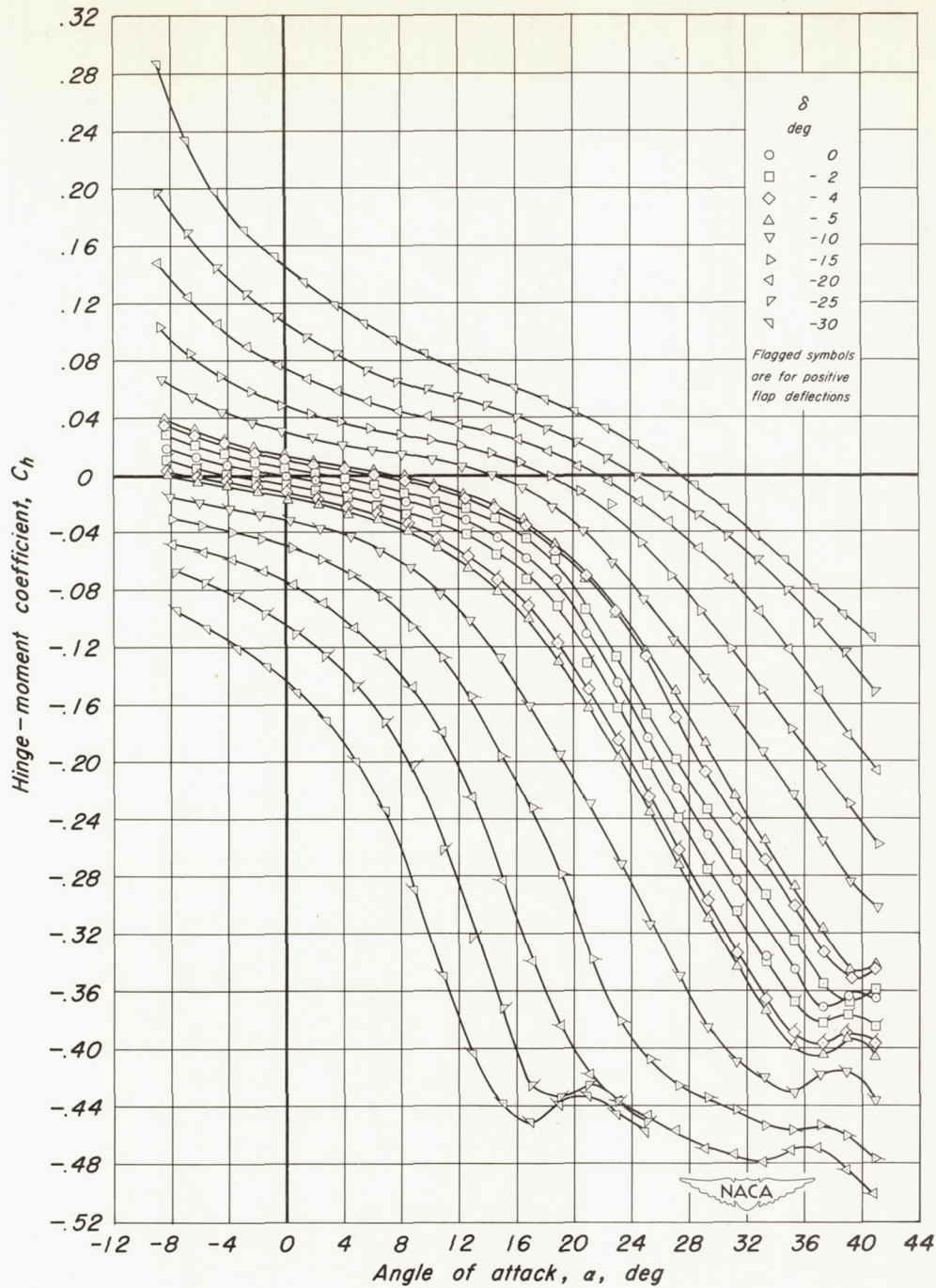
(c)  $C_h$  vs  $\delta$

Figure 7.—Concluded.



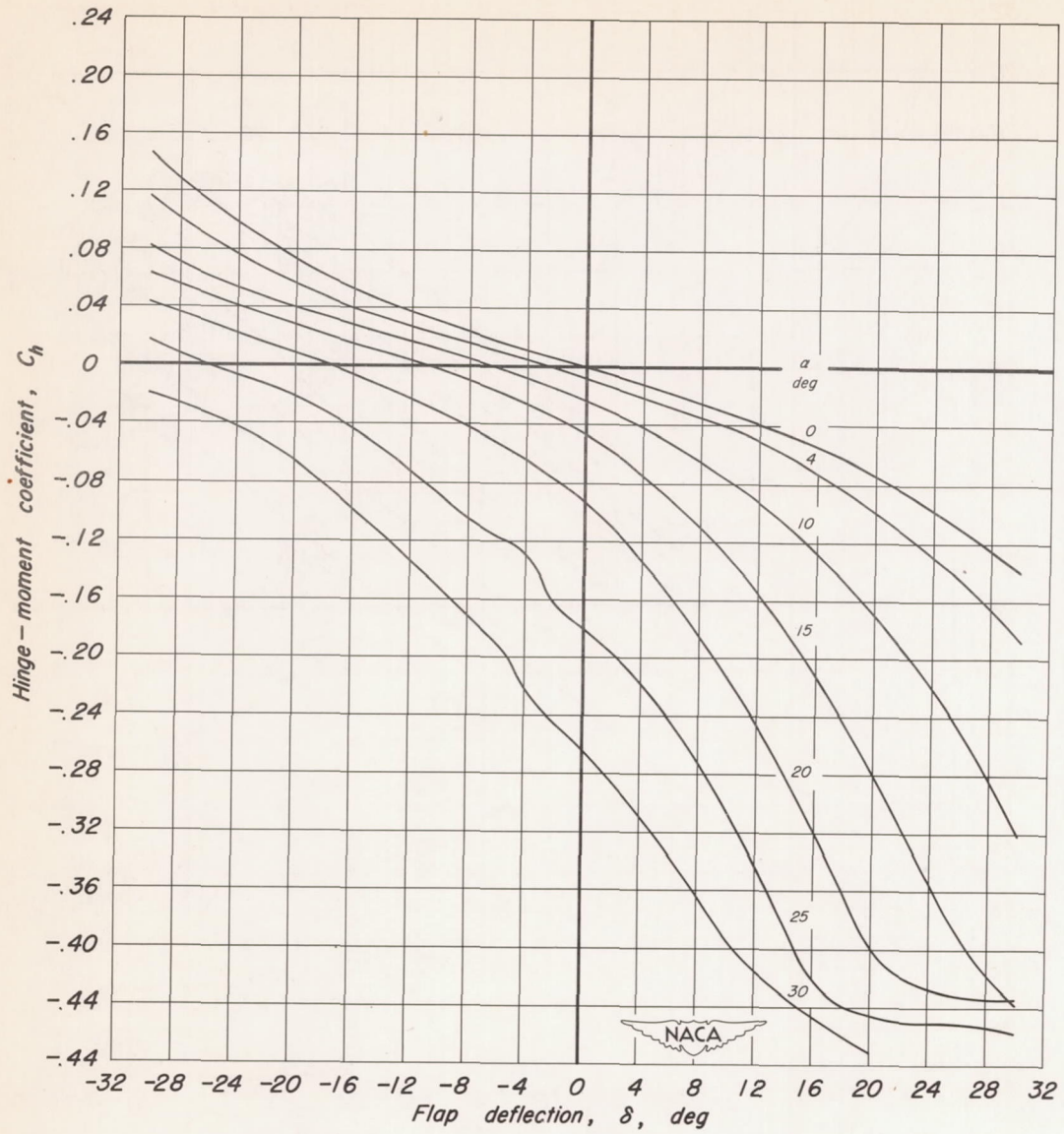
(a)  $C_L$  vs  $a$

Figure 8.- Lift and hinge-moment characteristics of horn-balanced control C on a triangular wing; 22.72 percent balance, normal contour horn, sealed, trailing-edge thickness,  $h/t=0$ .



(b)  $C_h$  vs  $a$

Figure 8.- Continued.



(c)  $C_h$  vs  $\delta$

Figure 8.- Concluded.

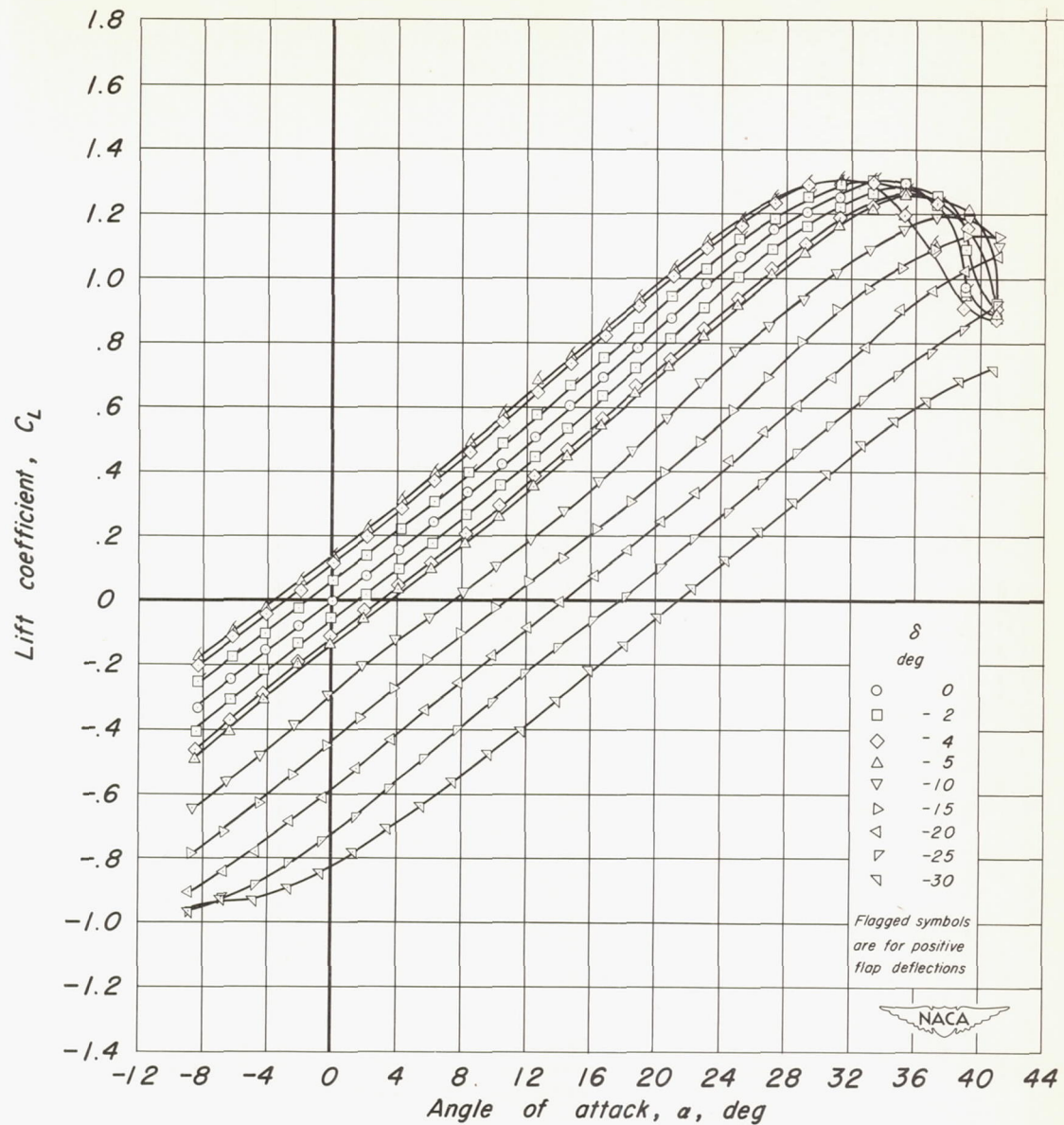
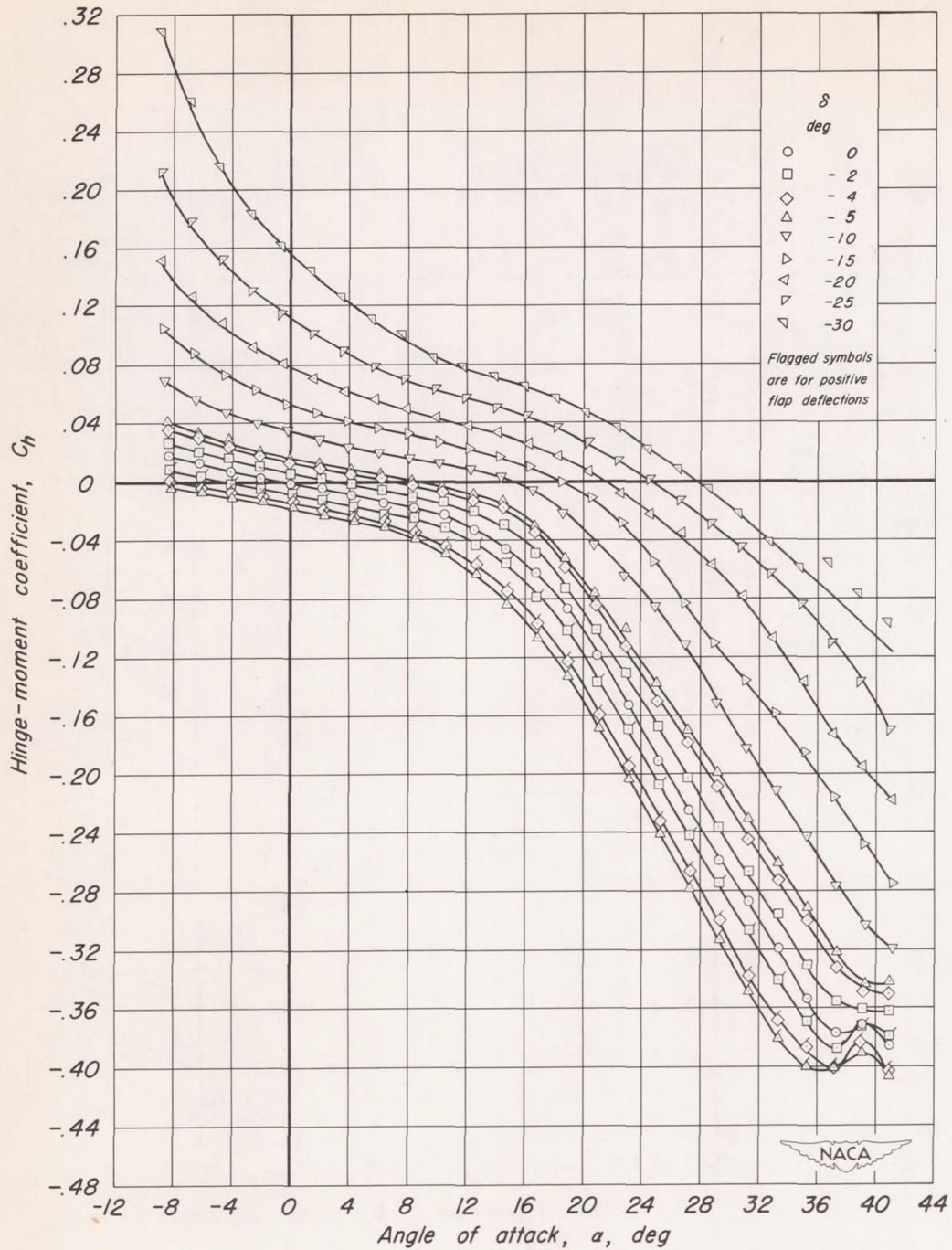
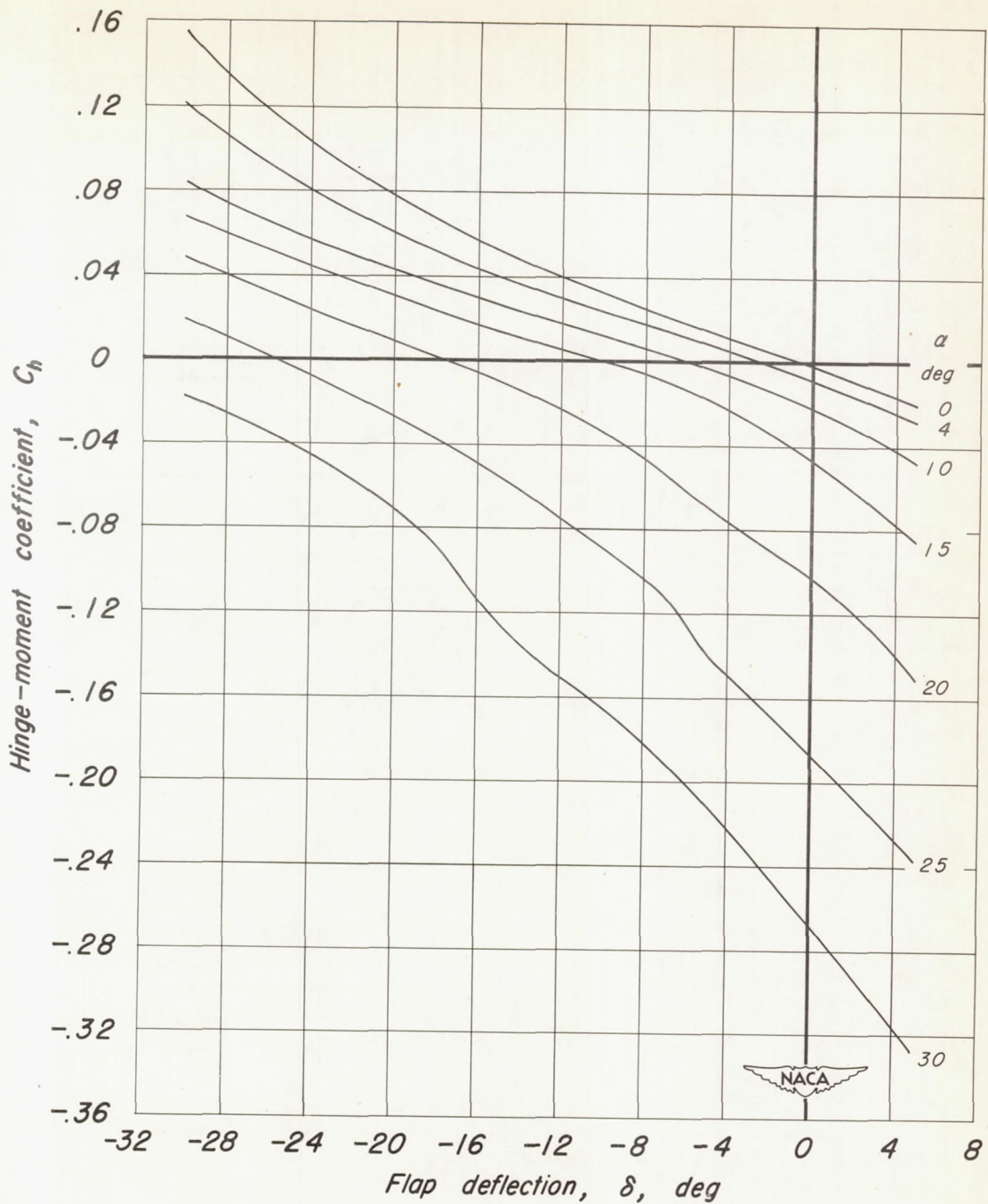
(a)  $C_L$  vs  $\alpha$ 

Figure 9.—Lift and hinge-moment characteristics of horn-balanced control C on a triangular wing; 22.72 percent balance, thin contour horn, sealed, trailing-edge thickness,  $h/t = 0$ .



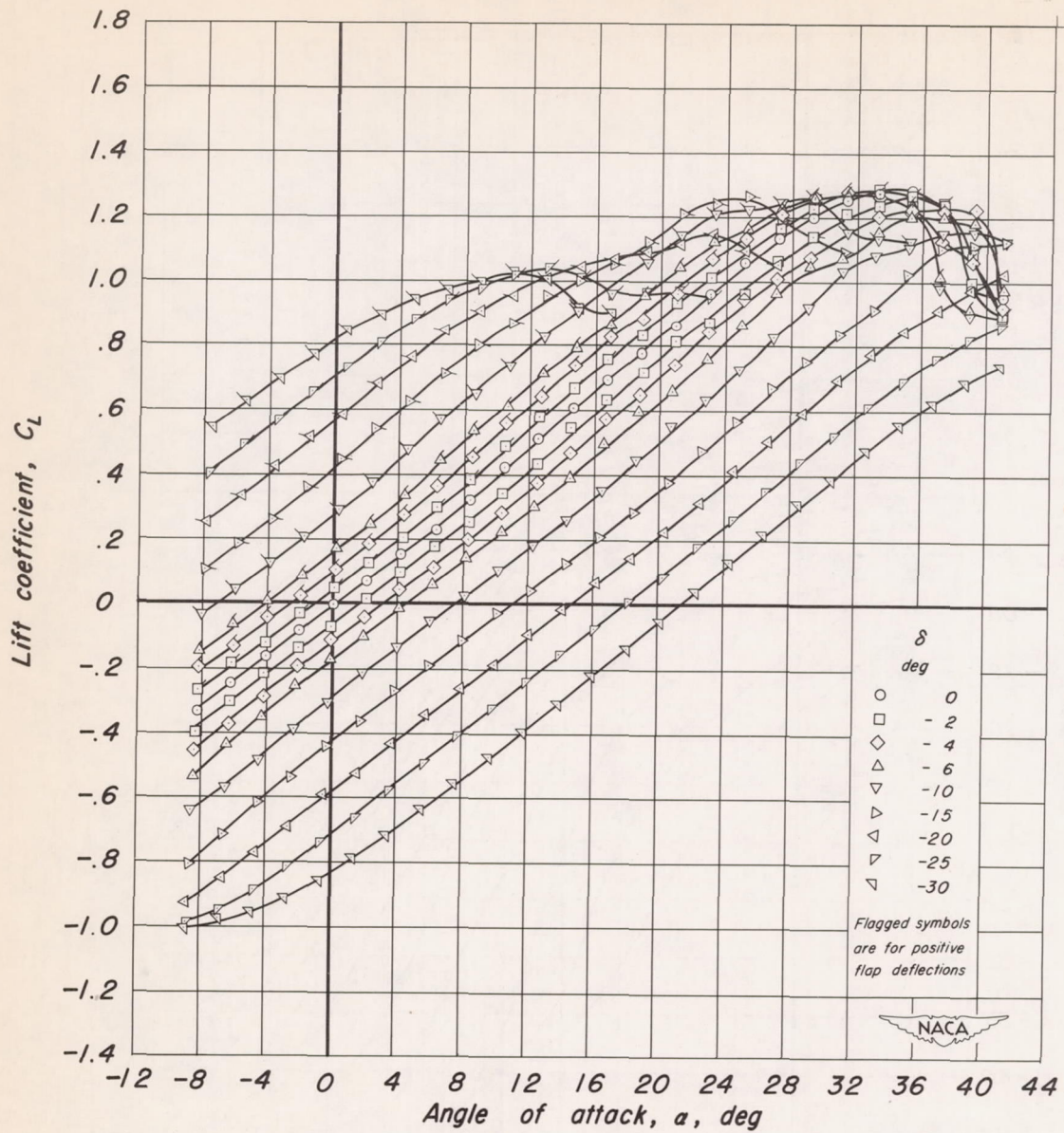
(b)  $C_h$  vs  $a$

Figure 9.-Continued.



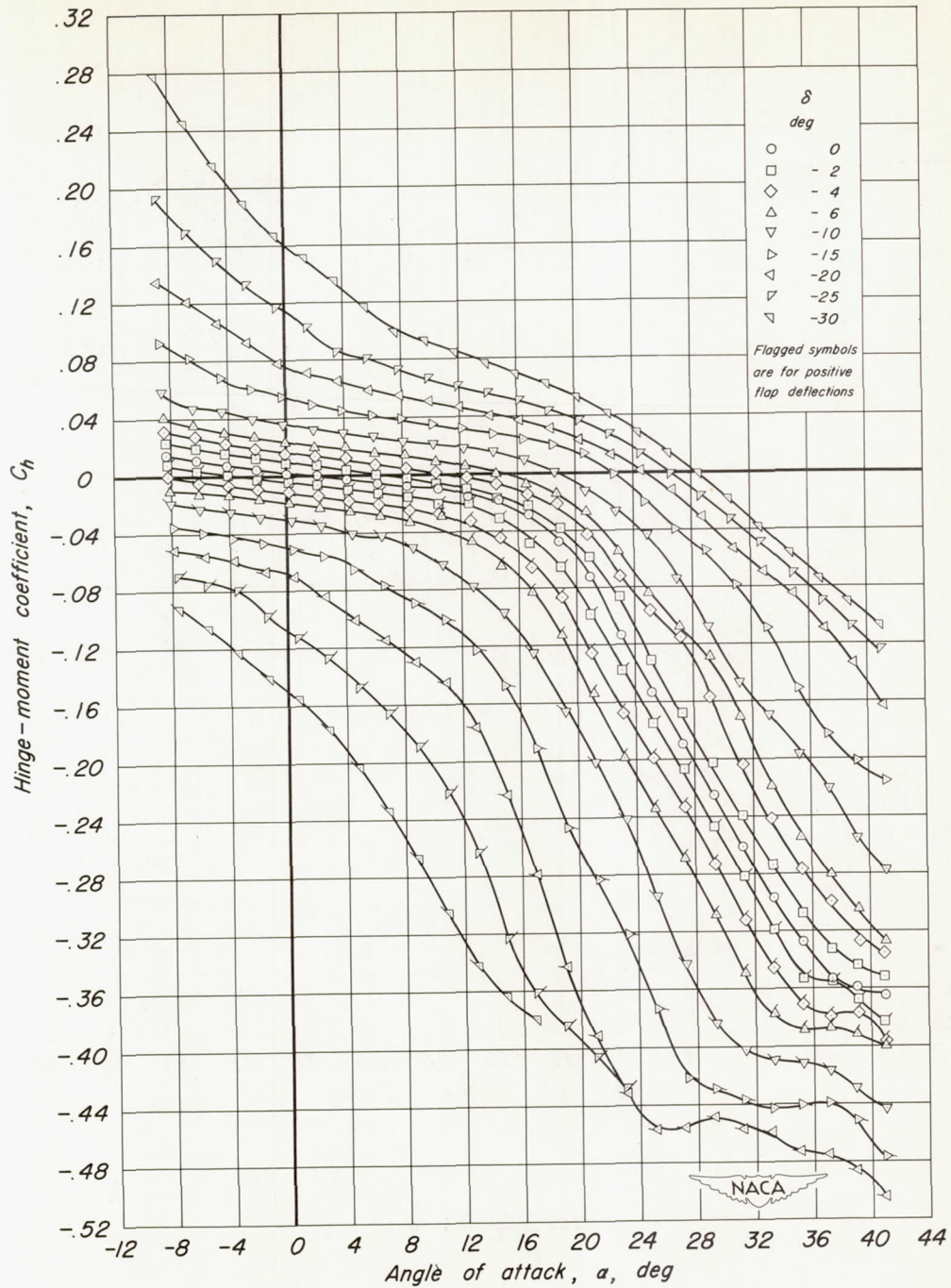
(c)  $C_h$  vs  $\delta$

Figure 9.-Concluded.



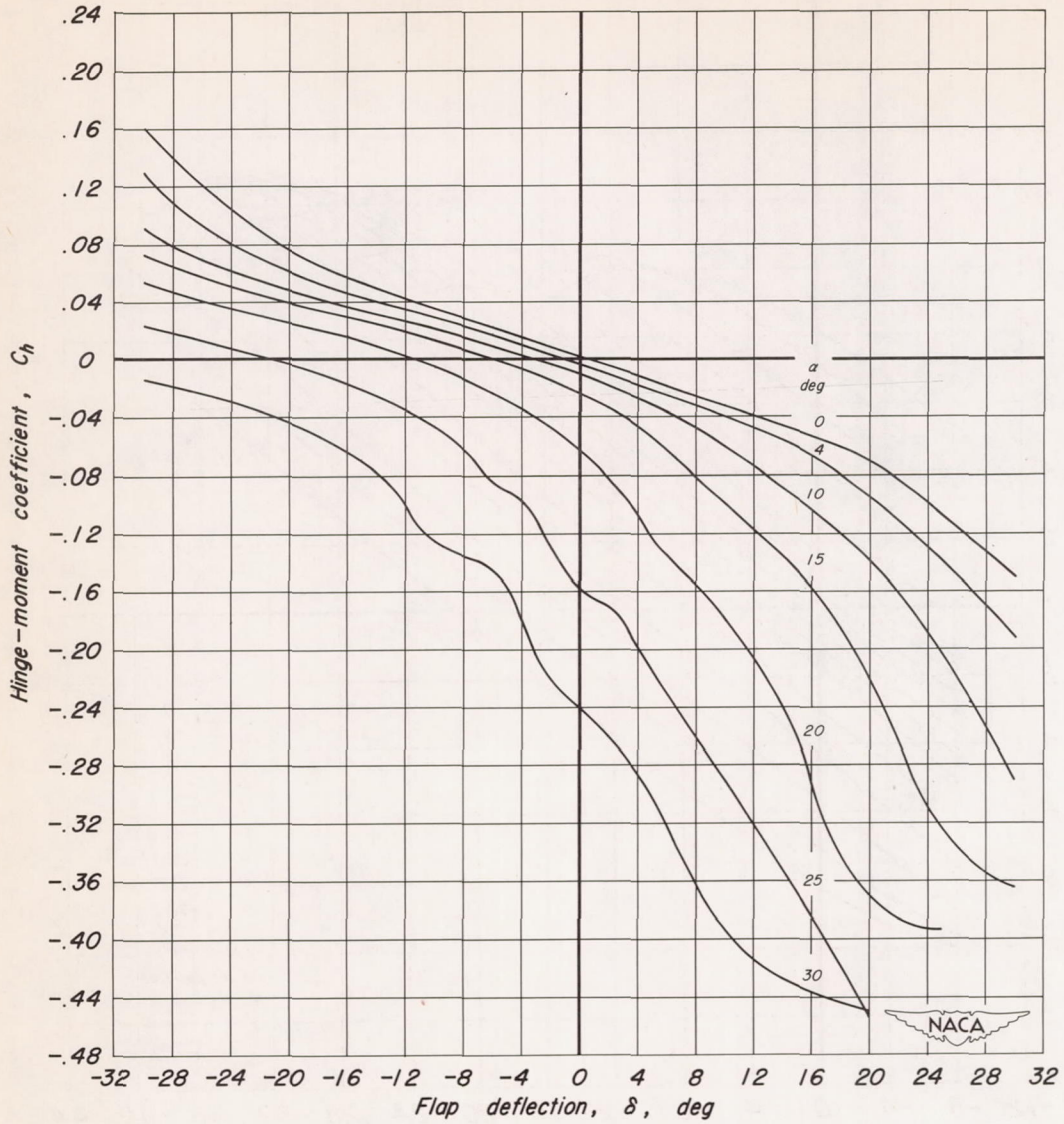
(a)  $C_L$  vs  $a$

Figure 10.—Lift and hinge-moment characteristics of horn-balanced control A on a triangular wing; 22.72 percent balance, normal contour horn, unsealed, trailing-edge thickness,  $h/t = 0.5$ .



(b)  $C_h$  vs  $a$

Figure 10.—Continued.



(c)  $C_h$  vs  $\delta$

Figure 10.- Concluded.

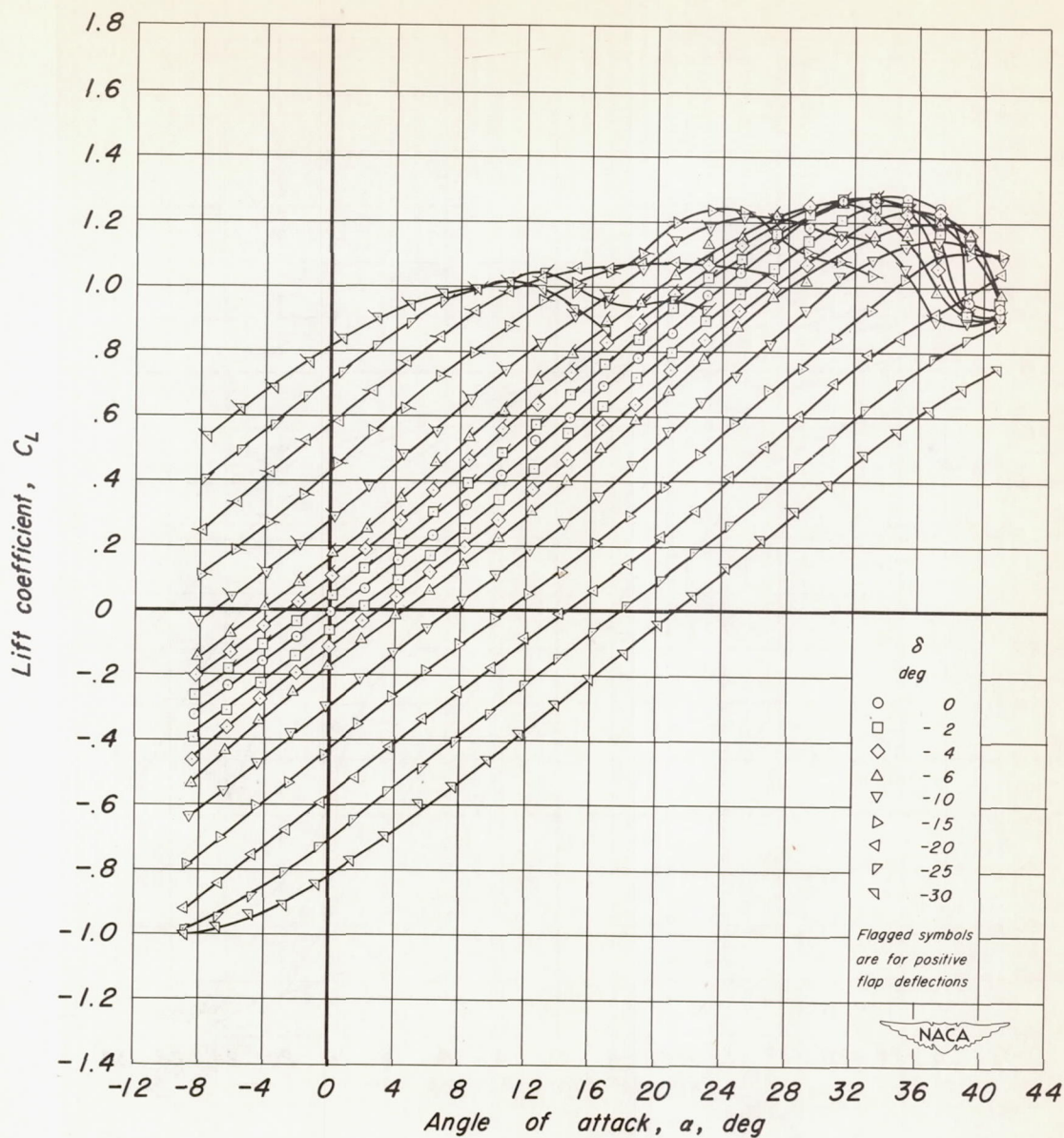
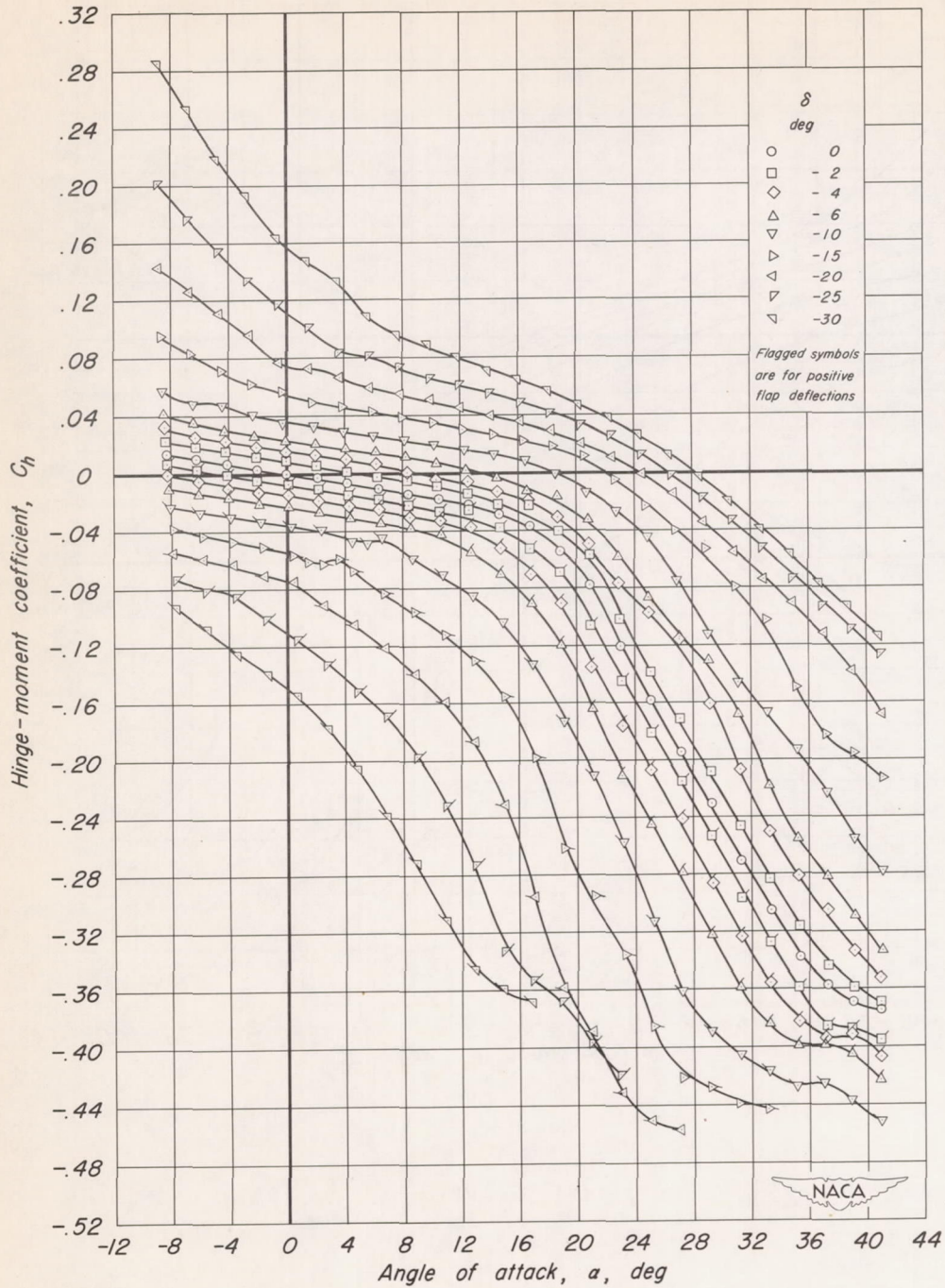
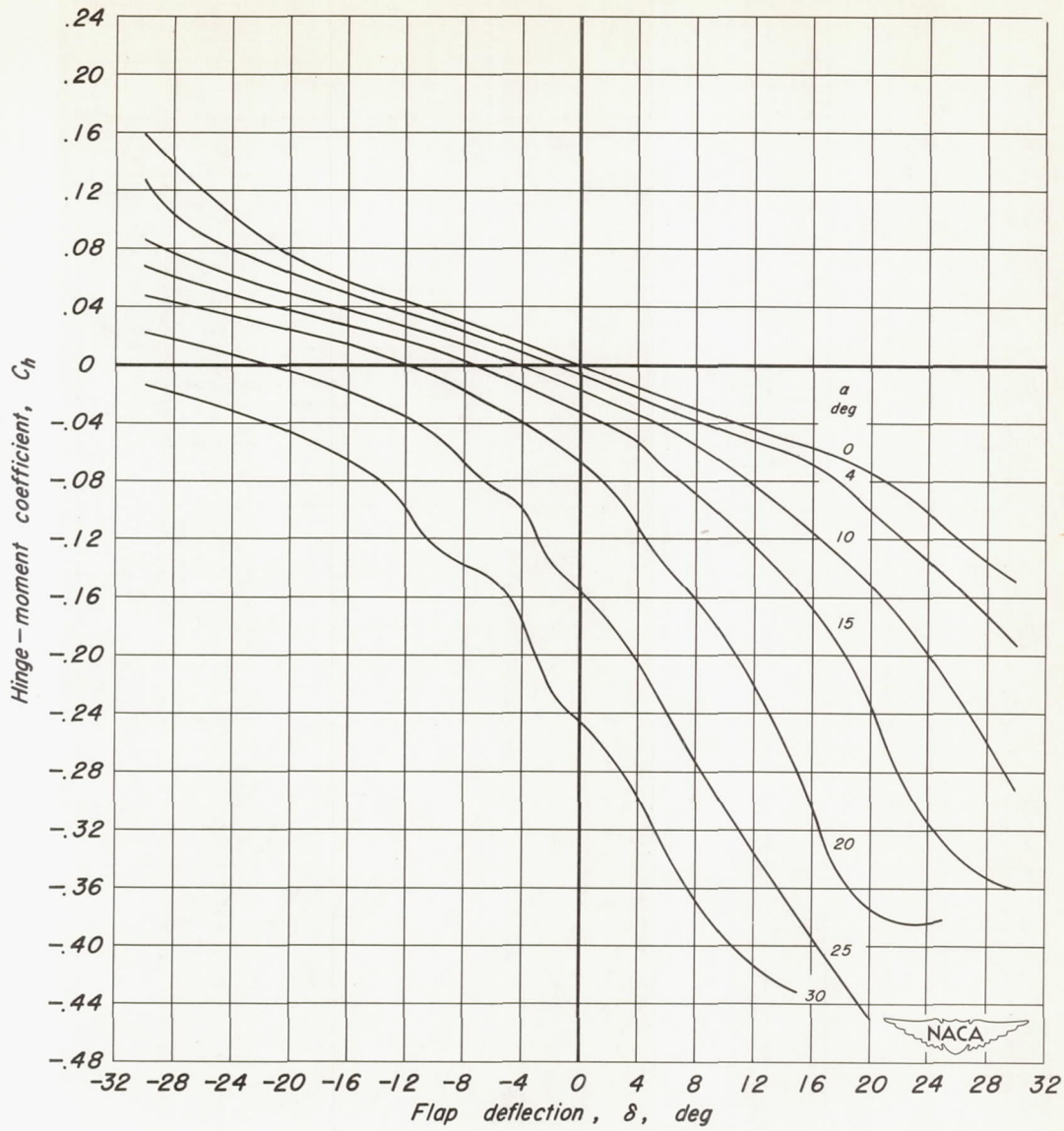
(a)  $C_L$  vs  $a$ 

Figure 11.— Lift and hinge-moment characteristics of horn-balanced control A on a triangular wing; 22.72 percent balance, normal contour horn, unsealed, trailing-edge thickness,  $h/t = 1.0$ .



(b)  $C_h$  vs  $a$

Figure 11.—Continued.



(c)  $C_h$  vs  $\delta$

Figure 11.-Concluded.

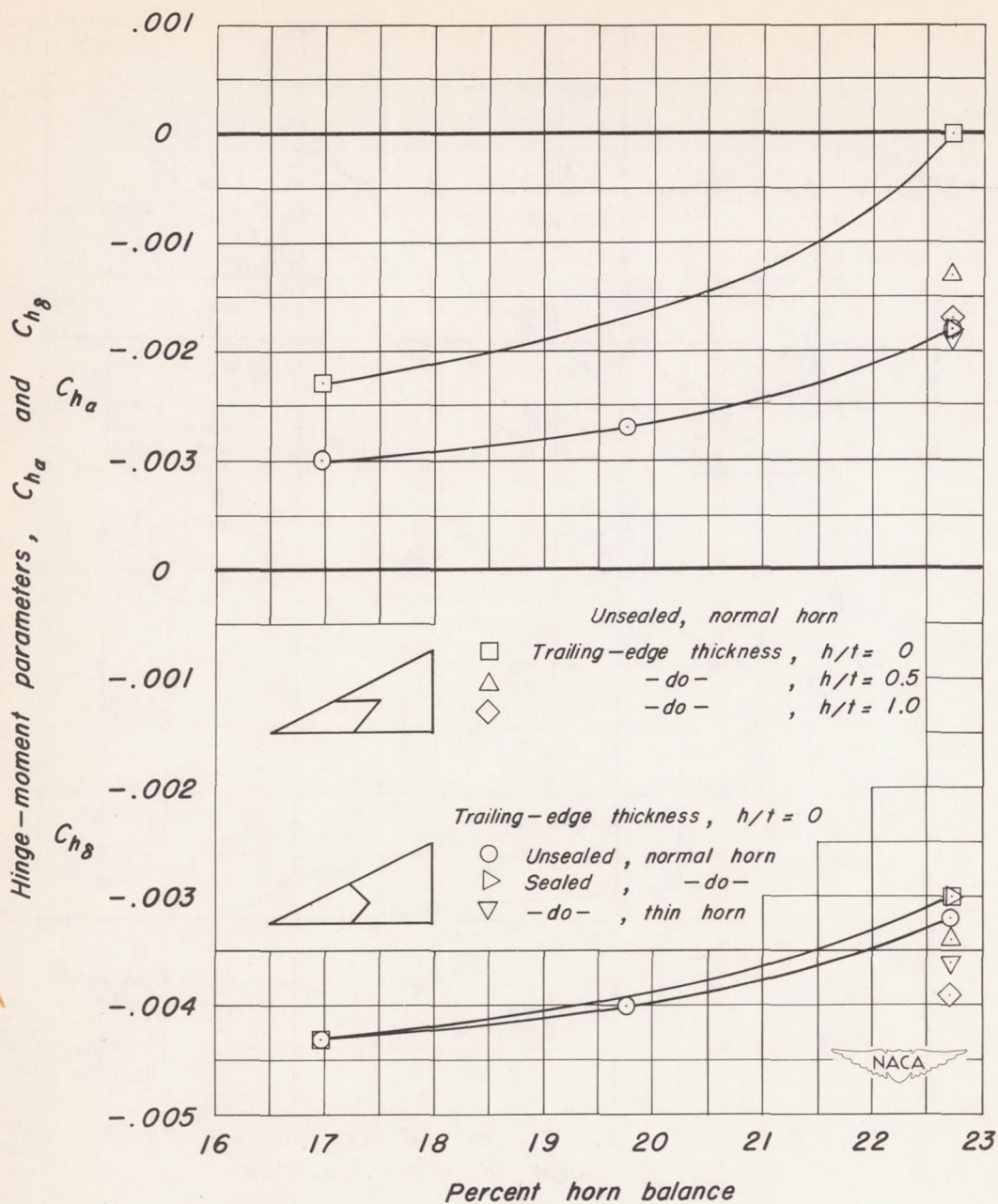


Figure 12.- The variation of the hinge-moment parameters with percent horn balance and the effect of trailing-edge thickness, flap nose seal, horn contour, and direction of horn gap for a constant-percent horn balance.

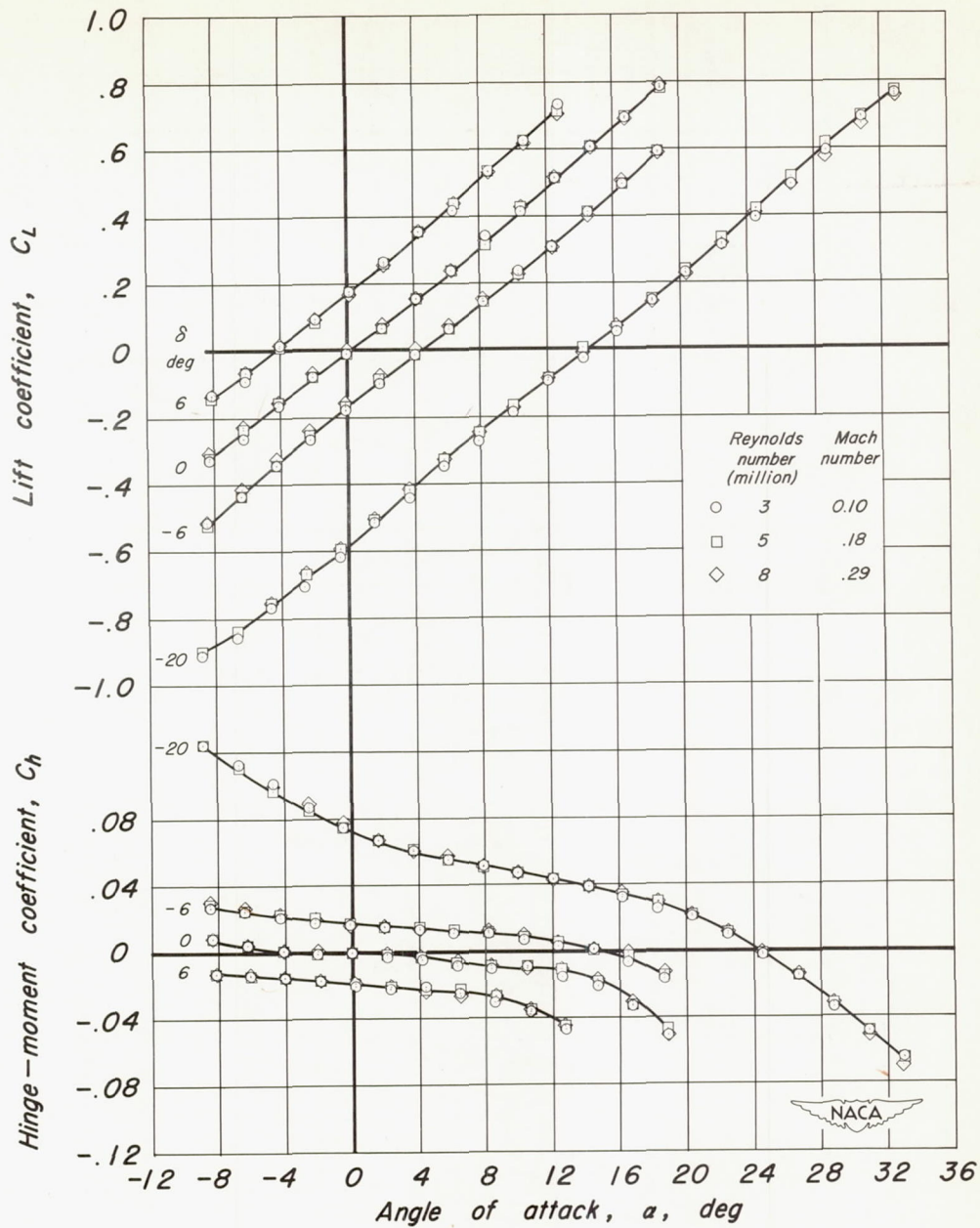
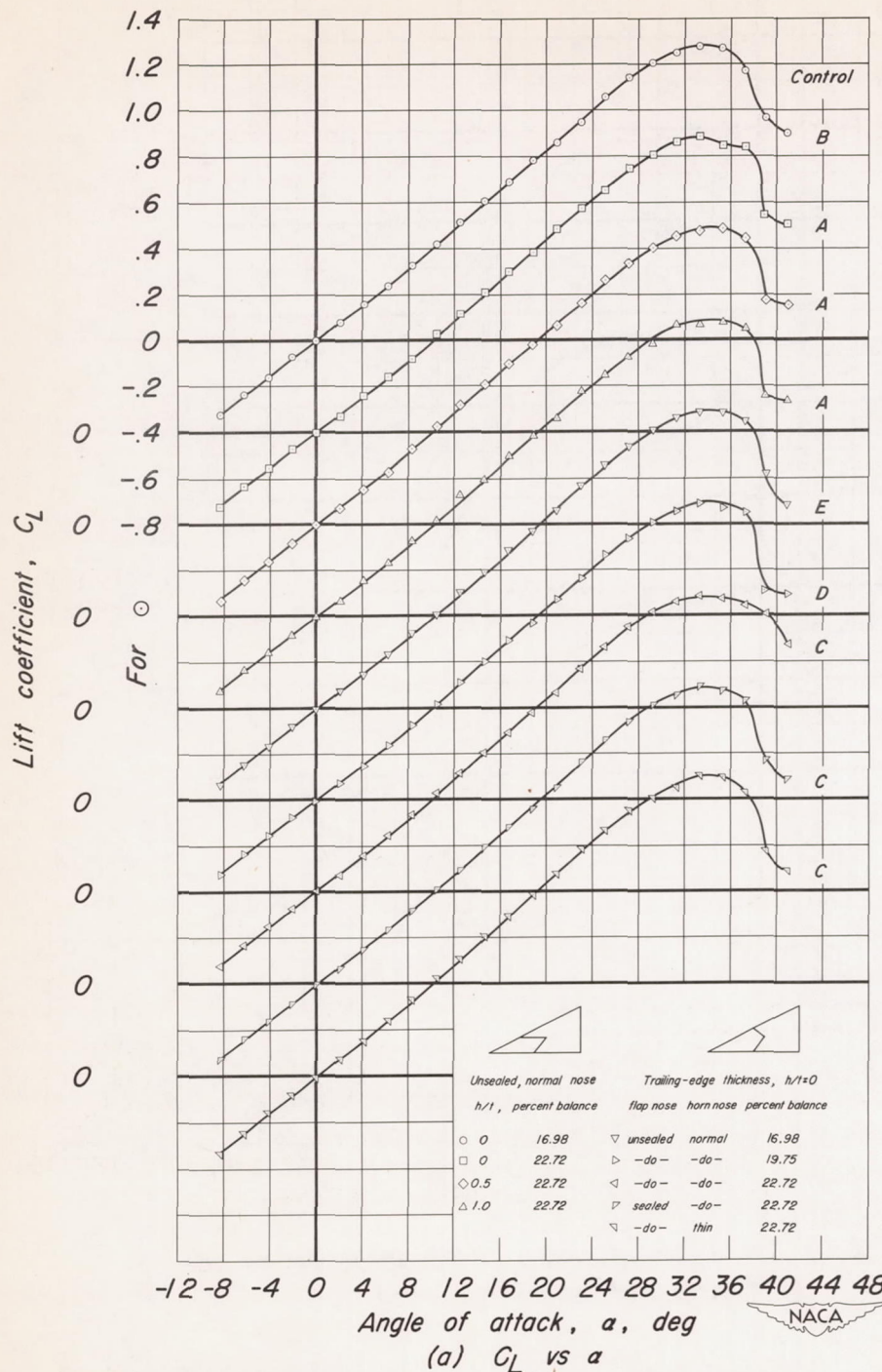
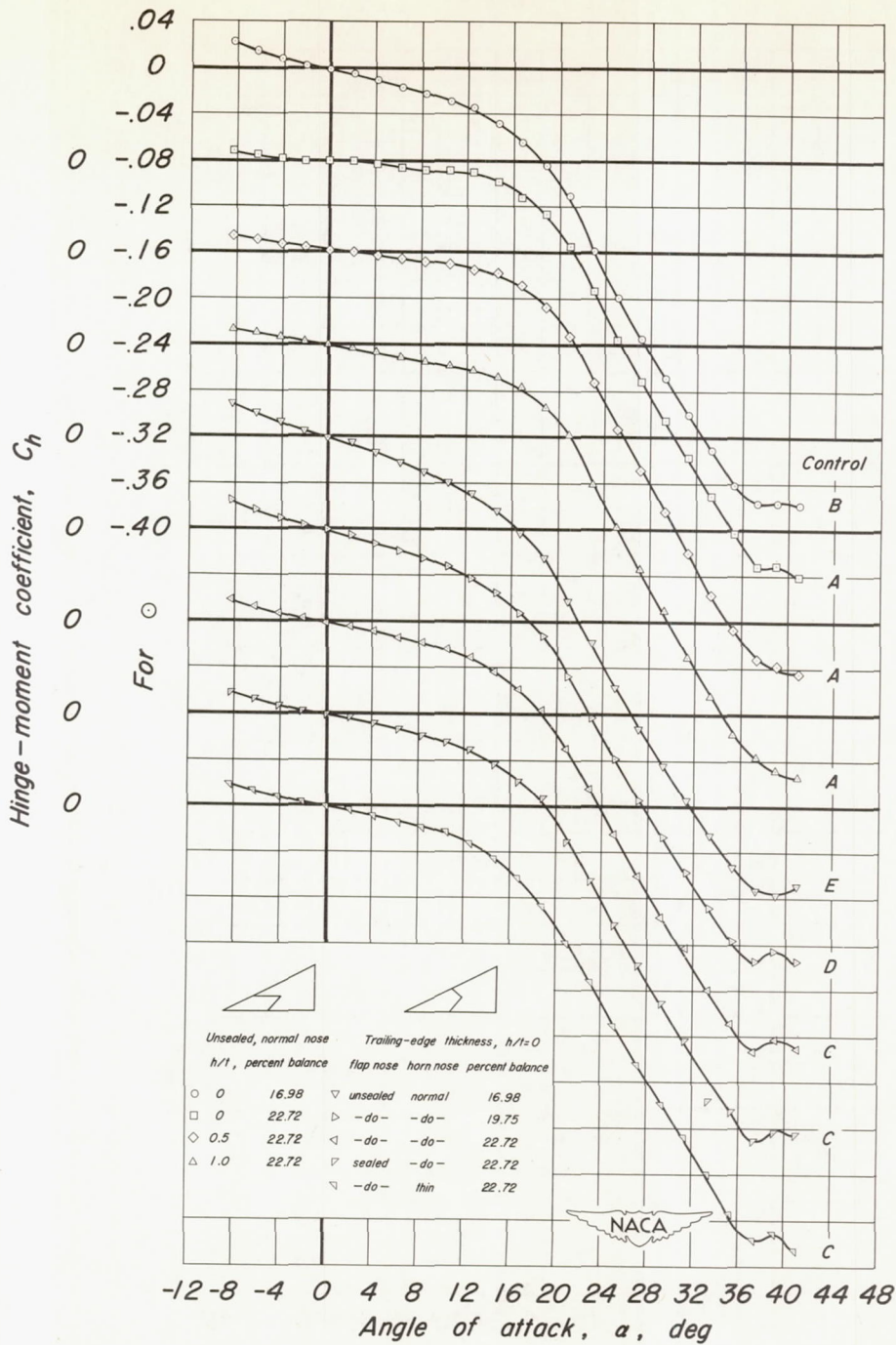


Figure 13.—The effect of Reynolds number on the lift and hinge-moment coefficients of control A ( $h/t=0$ ) on a triangular wing.



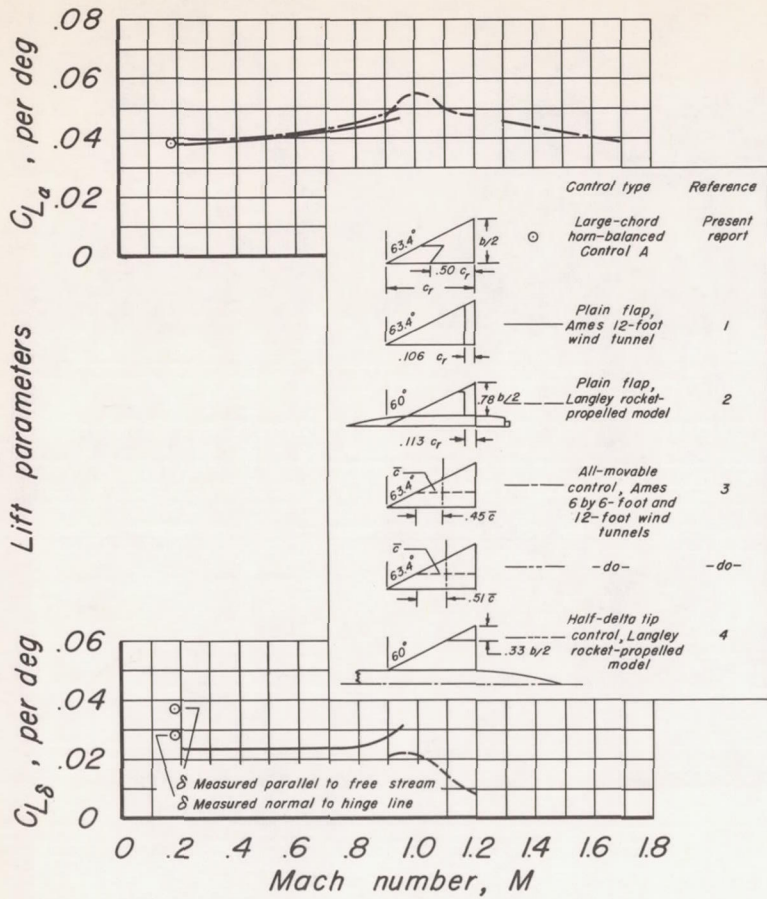
(a)  $C_L$  vs  $a$   
Figure 14.—A summary of the lift and hinge-moment coefficients of all of the controls tested on a triangular wing with the controls undeflected.



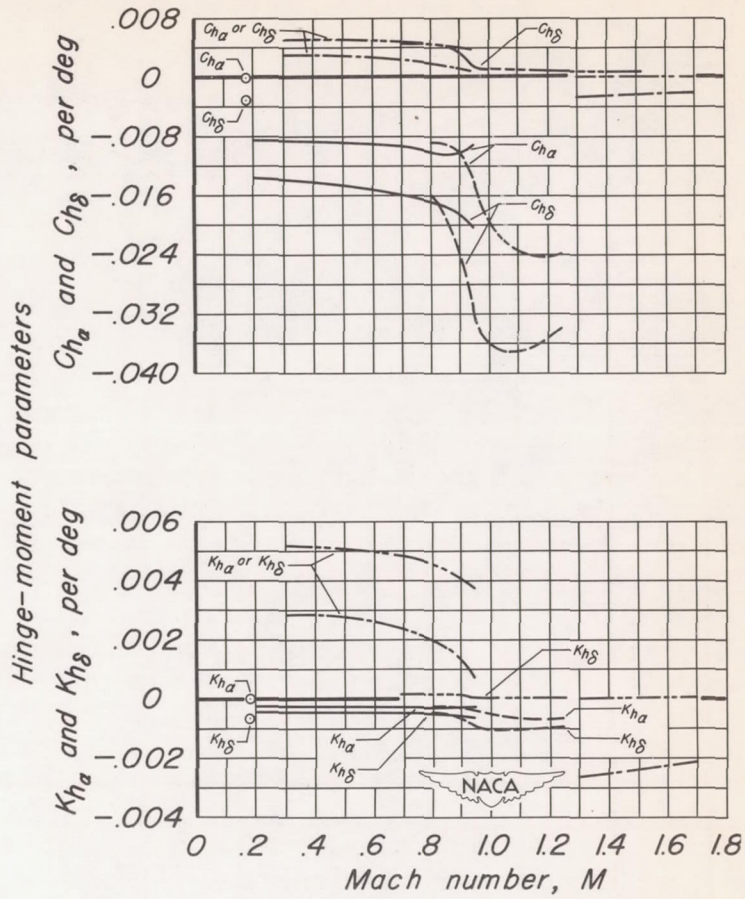
(b)  $C_h$  vs  $a$

Figure 14.—Concluded.

CONFIDENTIAL  
SECURITY INFORMATION



(a) Lift parameters.



(b) Hinge-moment parameters.

Figure 15.— A comparison of the lift and hinge-moment parameters of control A ( $h/t=0$ ) with several unbalanced and balanced controls.

CONFIDENTIAL  
SECURITY INFORMATION

SECURITY INFORMATION

CONFIDENTIAL

CONFIDENTIAL